

# MRO FTT/NAS & FLC

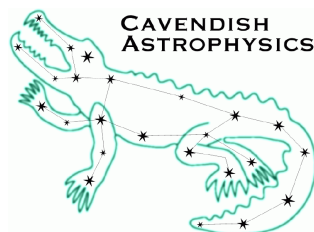
## FTT/NAS Preliminary Design Report

MRO-TRE-CAM-1100-0142

The Cambridge FTT Team

rev 1.2

30 April 2012



Cavendish Laboratory  
JJ Thomson Avenue  
Cambridge CB3 0HE  
UK

## Change Record

Revision	Date	Author(s)	Changes
0.1	2012-02-28	JSY	Initial Outline
0.2	2012-03-29	JSY	Converted to L <sup>A</sup> T <sub>E</sub> X, added Performance Evaluation
0.3	2012-04-22	CAH	First draft using words from many
0.4	2012-04-24	CAH	Revised structure
0.5	2012-04-26	CAH/MF	Revised words
0.6	2012-04-27	CAH/MF/DFB/JSY	Revised and more words
0.7	2012-04-29	CAH/MF	Revised all text save conclusions
0.8	2012-04-29	JSY	Revised all text, still no conclusions
0.9	2012-04-30	CAH	Added MF corrections
1.0	2012-04-30	JSY	Added conclusions, small edits
1.1	2012-04-30	JSY/EBS/DFB/XS	Small corrections
1.2	2012-04-30	JSY/MF	Small corrections

## Objective

To present the preliminary design of the FTT/NAS for the MROI Unit Telescopes.

## Scope

This document covers all optical, opto-mechanical, electronic and thermal aspects of the FTT/NAS. Software issues are dealt with in a separate partner document (AD2).

## Reference Documents

- RD1** Technical Requirements: Fast Tip-Tilt/Narrow-field Acquisition System (INT-403-ENG-0003) – rev 2.2, May 20th 2010
- RD2** Derived Requirements (MRO-TRE-CAM-0000-0101) — rev 1.0, August 31st 2010
- RD3** Technical Requirements: First Light Camera (INT-403-TSP-0107) – rev 1.0, May 20th 2010
- RD4** Technical Requirements: Unit Telescopes for the MRO Interferometer (INT-403-TSP-0003) – October 27th 2006
- RD5** Tyler, G.A., Bandwidth considerations for tracking through turbulence, JOSA, A, 11, pp.358-367 1994
- RD6** Nasmyth Table Space Envelope (INT-403-DWG-0100) – rev 0.5

## Applicable Documents

- AD1** Fast Tip-Tilt/Narrow-field Acquisition System Conceptual Design Report (MRO-TRE-CAM-0000-0102) – rev 1.1, August 31st 2010
- AD2** Fast Tip-Tilt/Narrow-field Acquisition System Software Preliminary Design Report (MRO-TRE-CAM-1160-0143) – rev 1.0, April 30th 2012

## Acronyms and Abbreviations

<b>AAS</b> Automated Alignment System	<b>FPGA</b> Field-Programmable Gate Array
<b>ADC</b> Atmospheric Dispersion Corrector	<b>FTTA</b> Fast Tip-Tilt Actuator
<b>AGN</b> Active Galactic Nucleus	<b>ICD</b> Interface Control Document
<b>AMOS</b> Advanced Mechanical and Optical Systems (UTM vendor)	<b>ISS</b> Interferometer Supervisory System
<b>BEASST</b> Back-End Active Stabilization of Shear and Tilt	<b>MROI</b> Magdalena Ridge Observatory Interferometer
<b>BCF</b> Beam Combining Facility	<b>NAS</b> Narrow-field Acquisition System
<b>CoDR</b> Conceptual Design Review	<b>NMT</b> New Mexico Tech
<b>CCCD</b> Charged Coupled Device	<b>PC</b> Personal Computer
<b>COTS</b> Commercial Off-The-Shelf	<b>PCI</b> Peripheral Component Interconnect
<b>CPU</b> Central Processing Unit	<b>PDR</b> Preliminary Design Review
<b>CTE</b> Coefficient of Thermal Expansion	<b>PSF</b> Point-Spread Function
<b>EIE</b> European Industrial Engineering (UTE vendor)	<b>ROM</b> Rough Order of Magnitude
<b>EMCCD</b> Electron-Multiplying Charge Coupled Device	<b>TBC</b> To be confirmed
<b>FEA</b> Finite-Element Analysis	<b>TBD</b> To be determined
<b>FTT</b> Fast Tip-Tilt	<b>UT</b> Unit Telescope
<b>FLC</b> First Light Camera	<b>UTE</b> Unit Telescope Enclosure
<b>FOV</b> Field-of-View	<b>UTM</b> Unit Telescope Mount

# Table of Contents

<b>1</b>	<b>Introduction</b>	<b>5</b>
1.1	MROI System Overview . . . . .	5
1.2	Top-level requirements . . . . .	8
1.3	Relationship between the FTT/NAS and the First Light Camera (FLC) . . . . .	8
<b>2</b>	<b>Derived Requirements</b>	<b>9</b>
2.1	Assumptions . . . . .	9
2.2	Pixel scale . . . . .	9
2.3	FTT mode sub-frame . . . . .	9
2.4	Image quality . . . . .	9
2.5	Stability of tip-tilt zero point . . . . .	10
2.6	Thermal management . . . . .	10
2.7	Closed-loop bandwidth . . . . .	11
2.8	Limiting sensitivity . . . . .	12
2.9	Dynamic range . . . . .	13
<b>3</b>	<b>FTT/NAS Design Overview</b>	<b>13</b>
<b>4</b>	<b>Optical Design and Layout</b>	<b>15</b>
4.1	Optical configuration and layout . . . . .	15
4.2	Optical component choices . . . . .	17
4.2.1	Dichroic . . . . .	17
4.2.2	Fold mirrors . . . . .	18
4.2.3	Focusing optic . . . . .	18
4.3	Throughput . . . . .	19
<b>5</b>	<b>Camera Selection</b>	<b>19</b>
<b>6</b>	<b>Opto-Mechanical Design</b>	<b>19</b>
6.1	Overall opto-mechanical architecture . . . . .	19
6.2	Key sub-assemblies . . . . .	20
6.2.1	Camera mount . . . . .	20
6.2.2	Optics baseplate . . . . .	23
6.2.3	Dichroic & fold mirror mounts . . . . .	25
6.2.4	Lens mount . . . . .	26
6.3	Mass budget . . . . .	26
<b>7</b>	<b>Thermal Design</b>	<b>27</b>
7.1	Thermal enclosure design . . . . .	27
<b>8</b>	<b>Electronics Design</b>	<b>29</b>
8.1	PC and electronics interface . . . . .	30
8.2	Services interface . . . . .	31
<b>9</b>	<b>Software Execution Environment</b>	<b>31</b>
<b>10</b>	<b>Testing Status and Results</b>	<b>31</b>
10.1	Camera readout testing . . . . .	32

10.2	Opto-mechanical testing . . . . .	32
10.2.1	Individual component testing . . . . .	33
10.2.2	Integrated testing . . . . .	36
10.3	Thermal testing . . . . .	38
<b>11</b>	<b>Lifetime and Maintenance</b>	<b>38</b>
11.1	Mechanical components . . . . .	38
11.2	Optical components . . . . .	39
11.3	Electronics components . . . . .	39
11.4	Camera . . . . .	39
<b>12</b>	<b>Interfaces</b>	<b>39</b>
12.1	Specific interface issues . . . . .	40
<b>13</b>	<b>Installation Procedure</b>	<b>40</b>
<b>14</b>	<b>Performance Evaluation</b>	<b>41</b>
14.1	Zero-point stability . . . . .	41
14.2	Closed-loop bandwidth . . . . .	42
14.3	Limiting sensitivity . . . . .	42
14.4	Mass budget . . . . .	43
<b>15</b>	<b>Conclusions</b>	<b>43</b>
15.1	Software . . . . .	43
15.2	Schedule and prospects . . . . .	44

# 1 Introduction

The FTT/NAS is one of a large number of opto-mechanical systems that comprise the Magdalena Ridge Observatory Interferometer. Although it is not the largest or most costly — these awards go to the delay-line system and the unit telescopes respectively — the role played by the FTT/NAS is a vital one. Before discussing how we envision that role might be satisfied, through an elaboration of our proposed design for the FTT/NAS, we provide below brief reviews of two key areas of technical background that are pertinent to the remainder of this document. The first focuses on how the FTT/NAS fits into the overall architecture of the MROI, while the second reiterates some of the most critical high-level requirements that the top-level science goals for the MROI have placed on the system. We hope that these preliminary paragraphs will provide valuable context for the reader, and make clearer some of the design decisions we have taken as we have converged towards our preferred design and implementation.

## 1.1 MROI System Overview

As in most astronomical optical/IR interferometers, the path from the location at which the light from a source is first intercepted by an individual UT to the place at which it is eventually detected is a long and complicated one (see Figure 1). This path can be conveniently described as involving a sequence of legs along each of which a collimated beam of light is transported between a pair of opto-mechanical systems. Each of these systems is responsible for conditioning the optical beam in some way or another prior to the beam being sent onto the next system. At the MROI this sequence of steps can be summarised by the entries in Table 1. This shows that the FTT/NAS is the third opto-mechanical assembly that the light from a target will meet on its path to the beam combiners. As its name suggests, its primary roles are two-fold:

1. To acquire the target — sensing its location in a wide field of view image and using the position of the target relative to a pre-determined location in the sensor field of view to provide signals to be used to adjust the pointing of the telescope;
2. Thereafter, to detect and eliminate rapid tip-tilt (i.e. angle of arrival) fluctuations in the incoming light beam due to atmospheric perturbations — sensing these by, again, measuring the position of the target relative to a pre-determined location in the sensor field and using these measurements to send high-frequency control signals to the active secondary mirror of the telescope and low-frequency pointing corrections to the UT mount.

The location of the FTT/NAS, on the Nasmyth table attached to the eastern-most end of each UT, was frozen during the early stages of the architecture of the MROI and so has not been considered as one of the degrees of freedom associated with the design task described in this document. Similarly, the decision to use dichroic separation to split the “short” wavelength light needed by the FTT/NAS from those wavelengths to be sent to the interferometric instrumentation was frozen at the same time (in order to maximise the interferometric throughput) and so has not been further assessed here either<sup>1</sup>.

Although the idea of, and methods for, controlling fast tip-tilt perturbations in an astronomical telescope are straightforward in concept, there are a number of critical differences between single-telescope and interferometer-based implementations that are worth identifying here. These principally relate to MROI-specific design choices and so may not be obvious to all readers.

- Although the primary roles enumerated above mention a “pre-determined” location on the FTT/NAS sensor, they do not explain how this fiducial “zero-point” is chosen and the process by which it is defined.

---

<sup>1</sup>The MROI Project Office has decided that initially the FTT/NAS sensor will use a bandpass from 600 nm to 1000 nm, but that once a visible light interferometric instrument has been installed (this is not expected until at least 2015, during Phase II of the project implementation) the bandpass from 350 nm to 600 nm must be available as a switchable alternative.

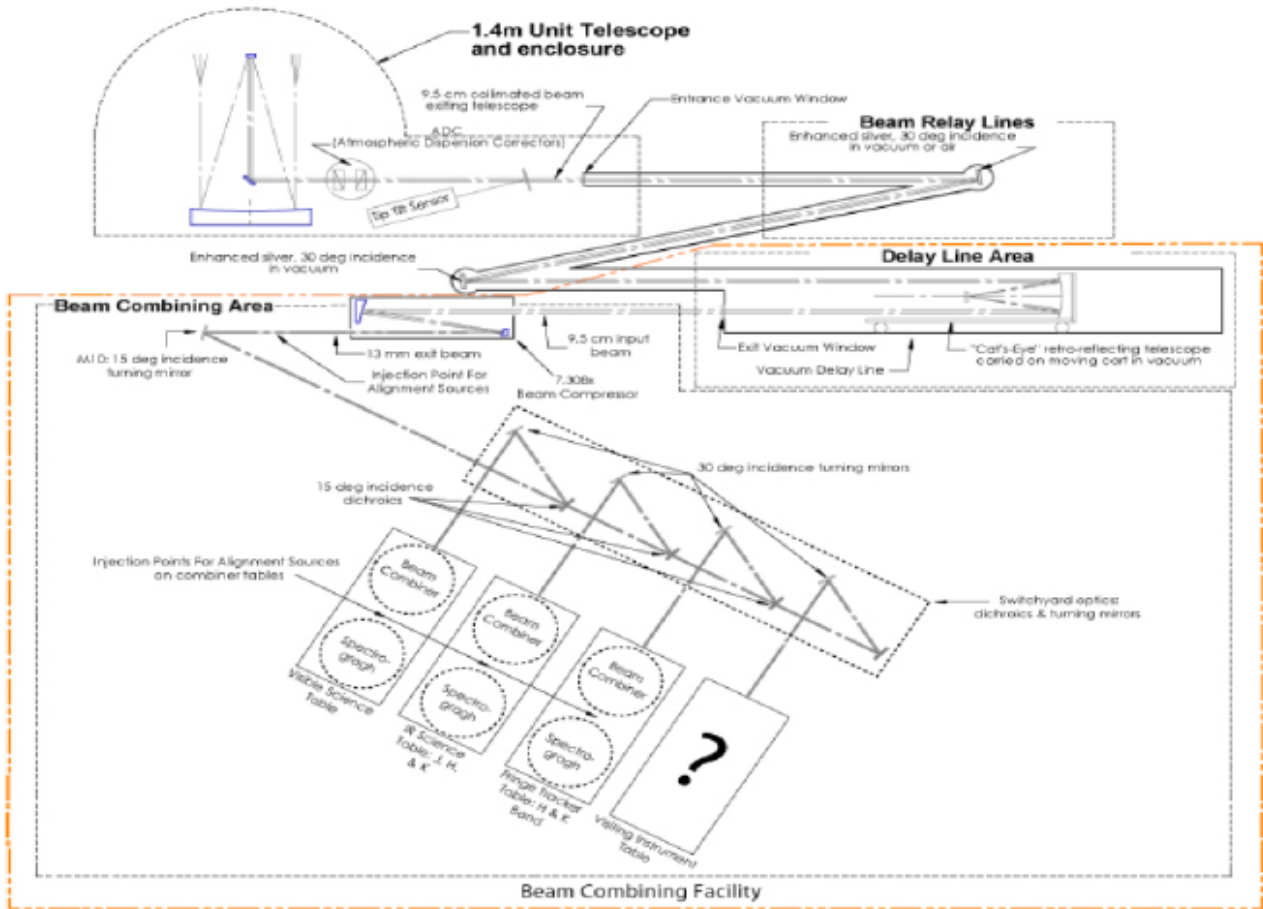


Figure 1: Illustration of the optical layout of the MROI showing the light-path from an individual UT (top left) to the beam combining instruments shown schematically at bottom left.

In fact, at the MROI this zero-point represents the guiding-centre (hereafter we shall refer to the guiding centre as the “objective-point”) on the FTT/NAS sensor which will guarantee that the light being sent to the beam combining laboratory will be delivered to the interferometric instruments<sup>2</sup>.

At the MROI, the location of the zero-point will be realised each night, prior to observing, by sending co-aligned and parallel light beams simultaneously to the interferometric instruments and to the UTs. The instruments in the beam combining laboratory will be aligned with respect to the inward-propagating beams, while at the UTs the outward propagating beams will be directed onto the FTT/NAS sensor after back-reflection from the FTT/NAS dichroic, retro-reflection off a corner-cube installed on the UT Nasmyth table and subsequent transmission through the FTT/NAS dichroic (see Figure 2 in Sec. 3).

Because it is a system goal to perform this registration of the zero-point only once per night, very stringent requirements have been placed on the stability of the optics through which the internal alignment beams are transmitted to each UT. Most of these optics will be located in the temperature controlled BCF, but two of them, the M4 and M5 mirrors, will be exposed to much larger temperature swings during the night: The median  $\Delta T$  between sunset and the coolest time of the night at the MROI site is 5 °C. In the system error budget the total two-axis allocation for uncontrolled jitter and slow drift for each of M4 and M5 is 0.015 seconds of arc (referred to the sky). We note that this is the same allocation given to the stability of the FTT/NAS zero-point due to any instabilities in its optics and sensor, and indeed the same

<sup>2</sup> More strictly, the zero point represents the objective-point for a target which is observed by the FTT/NAS and the interferometric instrument at the same wavelength, i.e. there is no differential atmospheric refraction between the guiding and science beams.

System	Component mirrors	System type (pass-thru or pickoff)	Input beam diameter (geometric)	Output beam diameter (geometric)	System primary role
Unit telescope	M1, M2, M3	Pass-thru	1400 mm	95 mm	Collects light and compresses beam
Atmospheric dispersion corrector	n/a	Pass-thru	95 mm	95 mm	Corrects for differential refraction between different colours
FTT/NAS	n/a	Pickoff	95 mm	95 mm	Diverts short wavelengths towards FTT/NAS sensor
Relay system	M4, M5	Pass-thru	95 mm	95 mm	Relays longer wavelengths towards BCF
Delay line system	M6 (twice), M7	Pass-thru	95 mm	95 mm	Adjusts optical path length of light beam
Beam compressor	M8, M9	Pass-thru	95 mm	13 mm	Compresses beam diameter
Beam turning mirror	M10	Pass-thru	13 mm	13 mm	Diverts beams towards correlator tables
Science switchyard	Dichroic and 1 or 2 mirrors	Pickoff	13 mm	13 mm	Diverts shorter wavelengths towards science correlator
Fringe tracker switchyard	3 mirrors	Pickoff	13 mm	13 mm	Reflects remaining longer wavelengths towards fringe-tracking correlator

*Table 1: Summary of sequence of optical systems that the light from the target follows as it passes from the unit telescopes to the science and fringe-tracking beam combiners.*

tilt stability requirement has been allocated to most of the other opto-mechanical systems enumerated in Table 1. We believe that this level of opto-mechanical stability is atypical for most FTT systems installed on single telescopes and much more stringent than is usual for those applications.

- An additional complication of the MROI FTT/NAS implementation is the fact that the light used for sensing the instantaneous position of the target image will be a different colour — in fact it will always be bluer — to that sent to the interferometric instruments. This is the reason that an Atmospheric Dispersion Corrector is the first system that light encounters after reflecting off the UT tertiary mirror (see Table 1). However, in its initial operational phase, the MROI Project Office has planned that an ADC will not be installed at each UT. As a result the objective-point on the FTT/NAS sensor will need to be deliberately offset from the zero-point established by the outgoing alignment beam from the interferometric laboratory to accommodate the difference in colour between the light being sent to the FTT/NAS sensor and that sent to the interferometric instrument. This atmospheric dispersion offset will be pre-computed by the Interferometer Supervisory System (ISS) based on the colours and elevation of the target and the bandpasses being sent to the FTT/NAS and interferometric instrument. Updated values will be made available to the FTT/NAS at a rate of approximately 0.1 Hz by the ISS.

In order to mitigate against uncertainties in the colours of the target source, the FTT/NAS is also required to permit small-angle synchronous dithering of the beam sent to the interferometric instruments so as to optimise the flux sent to them. Again, we believe this is a design feature not usually seen in single telescope FTT systems.

- Another feature of the FTT/NAS that relates to its role as a part of an interferometer (as opposed to any single telescope implementation) is the model that has been developed for its control. As for all the other interferometer systems, the operation of the FTT/NAS will be managed by the Interferometer Supervisory System. This will be responsible for sequencing all components of the array, for receiving

and publishing (where necessary) all telemetry and status data sent by the systems, and for providing ancillary information, for example dispersion offsets, to the array systems. This framework, however, also assumes that the individual systems will be largely “self-sufficient” and it is required that each system can operate and monitor its own performance independently. This level of in-built intelligence may be unusual when compared with other FTT installations.

- One final, and perhaps unusual, feature of the FTT/NAS procurement is that the active optical component of the system, the UT secondary mirror, will be supplied independently by AMOS (the UT vendor) and its sub-contractor Physik Instrumente. The performance of this component, and the related requirements associated with the FTT/NAS, have been carefully specified so as to allow for predictable performance of the complete closed-loop fast tip-tilt system when all its components are eventually integrated at the Magdalena Ridge.

## 1.2 Top-level requirements

The top level requirements associated with the FTT/NAS, and the less challenging requirements for the UT First Light Camera (FLC), are presented in detail in RD1 and RD3 respectively. The following brief list summarises some of the most critical of the FTT/NAS requirements:

- Management of time varying offsets due to atmospheric dispersion and/or off-axis guiding;
- Supporting the streaming of “live” diagnostic telemetry;
- Supporting a synchronous dither of the output beam direction;
- Supporting both acquisition and fast-guiding modes;
- Realising the sensitivity desired for faint-source science;
- Realising the zero-point stability requirements, especially in an exposed variable-temperature environment;
- Meeting the thermal dissipation budget;
- Designing a system that is compatible with the space constraints present on the Nasmyth optical table.

This is neither an exclusive nor ranked list, but serves simply to highlight some of the most challenging issues we have had to address as part of our preliminary design activity.

## 1.3 Relationship between the FTT/NAS and the First Light Camera (FLC)

It may be helpful to review here the relationship between the FTT/NA system and the FLC since these two sequential deliverables will share certain hardware and software. Apart for the relatively straightforward difference associated with the timing of their delivery — the FLC is expected to be ready roughly a year earlier than the complete FTT/NAS — the main distinction between these two systems will be their respective roles. The FLC has been designed primarily to facilitate acceptance testing, system integration, and evaluation of the UTs and the ISS, whereas the FTT/NAS will be responsible for providing the full functionality needed for acquisition and slow and fast guiding of the UTs during interferometric science observations. The Cambridge group have been charged with the design of both systems, but the FLC design is beyond the scope of this document. Notwithstanding this, we make a number of brief comments here:

1. We have designed the FLC software such that it will be possible to run it with the FTT/NAS hardware when the FTT/NAS is eventually delivered;

2. We intend to use some identical hardware elements for the FLC and FTT/NAS implementations. The most obvious example of this is the sensor head for both systems. We also expect to utilise identical optical mounts for some of the components of the two systems, although we will be using a less expensive achromatic optic to focus the FLC beam.

## 2 Derived Requirements

This section summarises the “derived requirements” and error budgets which apply to particular components of the FTT/NAS. These have been calculated from the top-level requirements specified in RD1, on the basis of our preferred design for the FTT/NAS. Only the results of the calculations are presented in this document; descriptions of the methods and reasoning used are provided in RD2.

### 2.1 Assumptions

In order to quantify the derived requirements it has been necessary to make certain assumptions about the design of the FTT/NAS. The main assumptions, which are consistent with our preferred implementation and have been used to obtain the specifications listed in several of the subsequent sections, were as follows:

- We have assumed that a single camera is used for target acquisition and fast tip-tilt sensing and that the same focusing optic is used to image the target onto the camera in all operating modes;
- We have assumed that the camera is an electron-multiplying CCD (EMCCD) with  $512 \times 512$  pixels and a read noise of 50 electrons RMS.

Further assumptions are described in the sub-sections below to which they apply.

### 2.2 Pixel scale

The pixel scale for the FTT/NAS shall be between 0.12 and 0.2 arc seconds per pixel. The lower limit is set by the NAS FOV requirement, and the upper limit is based on an assessment of the centroiding accuracy needed in FTT mode. Our proposed implementation satisfies this requirement with a pixel scale of  $0.15''$  per pixel.

### 2.3 FTT mode sub-frame

To allow for field rotation over a 300 second observation when using an off-axis tip-tilt reference, the fast tip-tilt mode sub-frame dimensions must be at least  $3.6'' \times 3.6''$ . For the range of pixel scales above, this sub-frame size corresponds to between 18 and 30 pixels square. Our proposed implementation using a 32 pixel sub-frame exceeds this requirement by a factor of 30%.

### 2.4 Image quality

To allow for accurate centroiding under the best seeing conditions expected, we require the PSF width to be no greater than one detector pixel. Table 2 presents a summary of the maximum allowed displacements on each of the optical elements for our proposed optical layout (see Sec. 4) that leads to a 50% encircled energy diameter no greater than the width of one detector pixel. These figures assume observations of a target at the edge of a 10 second of arc field of view, corresponding to the use of an off-axis tip-tilt reference object. The values in the table were obtained by constructing a ZEMAX model of the layout and perturbing each element in one

Element	Degree of freedom	Installation tolerance
Dichroic	$\delta z$	> 5 mm
	$\delta\theta_x$	0.37°
	$\delta\theta_y$	0.37°
Focusing optic	$\delta x$	> 5 mm
	$\delta y$	> 5 mm
	$\delta z$	0.35 mm
	$\delta\theta_x$	0.93°
	$\delta\theta_y$	0.93°
Fold mirror # 1	$\delta z$	0.17 mm
	$\delta\theta_x$	0.65°
	$\delta\theta_y$	1.9°
Fold mirror # 2	$\delta z$	0.22 mm
	$\delta\theta_x$	0.77°
	$\delta\theta_y$	1.2°
FTT/NAS sensor	$\delta z$	0.35 mm
	$\delta\theta_x$	> 5.0°
	$\delta\theta_y$	> 5.0°

*Table 2: Individual element tolerances in position and angle that lead to a 50% encircled energy diameter of greater than one pixel (16 microns) for our proposed optical layout (see Sec. 4). A focal length of 1525 mm has been assumed. For each element the z-coordinate represents the direction normal to the plane (or optical axis) of the component, while the x- and y-axes are orthogonal to this with the x-direction perpendicular to the Nasmyth table.*

degree of freedom at a time until the 50% encircled energy diameter increased above one pixel i.e. 16  $\mu\text{m}$ . An observing wavelength of 600 nm was assumed.

These tolerances are all relatively large and so we expect it will be straightforward to install the FTT/NAS optics to this level of absolute precision on the Nasmyth optical table.

## 2.5 Stability of tip-tilt zero point

Table 3 shows the error budget for the maximum allowable component displacements that meet the top-level zero-point stability budget for our proposed optical layout. These numbers are much smaller than those associated with the image quality budget for the FTT/NAS optics, and so identify component stability, rather than absolute orientation, as the key challenge for the opto-mechanical design for the FTT/NAS.

## 2.6 Thermal management

We have refined the derived requirements presented in RD2 to accommodate our latest knowledge of the heat dissipation of the candidate EMCCD camera and the top-level heat dissipation requirements. Our modelling (and design) assumes that the FTT/NAS sensor is placed inside an environmentally-controlled enclosure and in particular that:

- When operating at night the camera enclosure temperature is controlled to protect the camera and to minimise heat dissipation to the environment, and to ensure that the outer surface temperature of the camera enclosure is within 2 °C of ambient;

Element	Degree of freedom	Allocation to global stability budget
Dichroic	$\delta\theta_x$	0.047''
	$\delta\theta_y$	0.045''
Focusing optic	$\delta x$	0.47 $\mu\text{m}$
	$\delta y$	0.35 $\mu\text{m}$
	$\delta z$	140 $\mu\text{m}$
	$\delta\theta_x$	0.75''
	$\delta\theta_y$	0.70''
Fold mirror # 1	$\delta z$	0.59 $\mu\text{m}$
	$\delta\theta_x$	0.090''
	$\delta\theta_y$	0.049''
Fold mirror # 2	$\delta z$	0.31 $\mu\text{m}$
	$\delta\theta_x$	0.064''
	$\delta\theta_y$	0.074''
Camera mount	$\delta x$	0.47 $\mu\text{m}$
	$\delta y$	0.35 $\mu\text{m}$
	$\delta z$	140 $\mu\text{m}$
	$\delta\theta_z$	2.32''

*Table 3: The stability budget allocations for our proposed optical layout for the FTT/NAS. In each case the optic must not move by more than this amount for a 5 °C change in temperature. The co-ordinate system used has the z-direction normal to the named optical component, and the x- and y-directions perpendicular to this. In all cases, the x-direction is perpendicular to the surface of the Nasmyth optical table, and the figures represent "displacements" with respect to the symmetric expansion of the whole opto-mechanical layout.*

- The camera environment is controlled at all times (assuming power is not interrupted), even though the camera may not be switched on. This will ensure that the camera can be switched on without first having to warm up or dry the enclosure;
- The camera enclosure contains a heating element so that the enclosure can be warmed up after a long power break during cold weather and to prevent the enclosure being too cold when the ambient air temperature is increasing;
- The air in the camera enclosure is maintained above the dew point whenever the camera is powered on (and preferably at all times so as to reduce the risk of condensation on the internal electronics);
- That heat is removed from the camera Peltier heat exchanger and the enclosure via the use of a liquid flowing at a controlled temperature and rate.

Under these assumptions the latest versions of the derived thermal requirements are shown in Table 4.

## 2.7 Closed-loop bandwidth

If one assumes a frame rate of 1 kHz and a total compute latency of 100 microseconds, then a maximum readout latency (defined as the delay from the end of exposure to the pixel data being available for processing) of 1130 microseconds is needed to meet the requirement for a 40 Hz closed-loop 3dB bandwidth. To meet a 50 Hz bandwidth goal, the maximum readout latency that can be tolerated is 790 microseconds. As will be seen later, our proposed design is able to meet the requirement.

Item	Latest requirement	Change since CoDR
Maximum enclosure internal air temperature	30 °C	
Minimum enclosure internal air temperature	0 °C	
Minimum enclosure internal air/ external surface temperature differential	3 °C (Goal 8 °C)	
Enclosure air dew point	Coldest enclosure internal component -5 °C	
Enclosure residual heat dissipation	6 W	Increased from 5 W
Emissivity of outer surface of enclosure	> 0.7	
Residual camera heat dissipation	12 W	Decreased from 20 W
Camera enclosure space envelope	340 mm (w) × 320 mm (d) × 350 mm (h)	Was 340 mm × 300 mm × ≤ 350 mm
CPU and interface power dissipation allowance	190 W	
Camera interface and controller power dissipation allowance	70 W	
Power consumption allowance	250 W	

Table 4: Summary of derived thermal requirements for the FTT/NAS. Only small changes have occurred since CoDR.

## 2.8 Limiting sensitivity

Table 5 gives the tip-tilt residual error budget for an observation of a  $m_v = 16$  active galactic nucleus (AGN), with the red colours defined in RD1, under the conditions specified in that document. We have assumed a closed-loop bandwidth of 15 Hz, optimal for the specified seeing. The UT tilt residuals are from RD4 (but note that these values were specified at 10 Hz bandwidth — the true values for 15 Hz bandwidth could be up to 33% lower, i.e. better). The residual seeing tilt was calculated using the results from Tyler (1994, RD5).

Tilt error	RMS error/mas	Origin
UT residual mount error	20	RD4
UT residual wind shake	30	RD4
Residual seeing tilt	30	RD5
Speckle noise centroiding error	15	See text
Detection noise centroiding error	34	See text
Total	60	

Table 5: The two-axis tip-tilt error budget in seeing conditions of  $r_0 = 14$  cm and turbulent layer wind speed  $V = 10$  m/s.

The speckle noise centroiding error is a bias that varies from frame to frame due to the centroiding algorithm not properly accounting for the multiple speckles making up each short exposure image. The magnitude of this effect will depend on the precise centroiding algorithm used, the choice of which will be investigated in the

post-PDR phase. For now we have adopted an intermediate value between that for conventional centre of mass algorithms and that for thresholded centre of mass algorithms.

We derive an allocation of 34 milliarcseconds for the two-axis “detection noise” centroiding error (the combined effects of photon shot noise and detector readout noise). Given realistic assumptions about the atmospheric, UT and camera window optical throughput and the CCD quantum efficiency, and assuming negligible read noise, we require the other FTT optics (dichroic, focusing optic, fold mirrors) to have 102% throughput. Hence we believe that the limiting sensitivity requirement cannot quite be met.

If we conservatively assume 85% throughput for these FTT optics, the total residual tilt will then be roughly 2% over budget. This would result in an additional visibility loss in the H-band of merely 0.5% over what has been budgeted.

The detector read noise will have negligible performance impact (1% degradation of the centroiding accuracy) as long as the effective read noise remains below 0.20 electrons per pixel, assuming a  $6 \times 6$  pixel quad cell. This implies electron multiplication gains of at least 250 for an EMCCD with an output read noise of 50 electrons.

## 2.9 Dynamic range

We expect that that the FTT mode frame rate will be 1 kHz except for the very faintest stars. Our design also permits that in the NAS mode the exposure time will be adjustable independently of the frame rate and that a minimum exposure time of 1 millisecond can be realised.

Under these assumptions, just two EMCCD amplification settings — corresponding to the use of no gain and a sufficiently high gain to reach the limiting sensitivity — can be used to allow observations spanning the magnitude range from 3.3 to 16 (in good seeing), for both FTT and NAS modes. Stars as bright as magnitude 1.8 can be observed in poor seeing. There is a 2-magnitude overlap between the faintest objects observable without amplification and the brightest objects observable with amplification, hence it should usually be possible to observe a science target and calibrator with the same gain setting. These magnitudes correspond to the red target colours specified in RD1, which are appropriate for AGN and red supergiant stars. Observations of brighter targets will require the use of a pupil mask or neutral density filter to prevent the camera from saturating.

## 3 FTT/NAS Design Overview

In this section we present a high-level overview of our proposed FTT/NAS design and outline the reasoning that has led us to select this system architecture. Our implementation (see Figure 2) is based around a COTS back-illuminated EMCCD camera (Andor iXon X3 897, formerly branded as the iXon<sup>EM</sup> + 897), which offers fast readout, high quantum efficiency and sub-electron effective read noise, all of which are needed to meet the stringent closed-loop bandwidth and limiting magnitude requirements of the FTT/NAS. Images from the FTT/NAS sensor will be interrogated by a local computer which will serve to both archive the data (either locally or via the ISS) and to send control demands to the secondary mirror FTT actuator controller. Information on the current state of the UT mount, and any ancillary information needed by the FTT/NAS will be delivered via the ISS.

We have chosen to use the same sensor for both target acquisition and fast tip-tilt correction, with a fixed pixel scale. This implies a sufficiently large-format camera to satisfy the  $60 \times 60$  arc second field-of-view requirement. A minimum of 2.5 pixels across the short-exposure image FWHM is considered necessary for accurate centroiding (RD2), this pixel scale constraint leading to a minimum CCD format of 500 pixels. Our choice of camera and pixel scale satisfy both these needs.

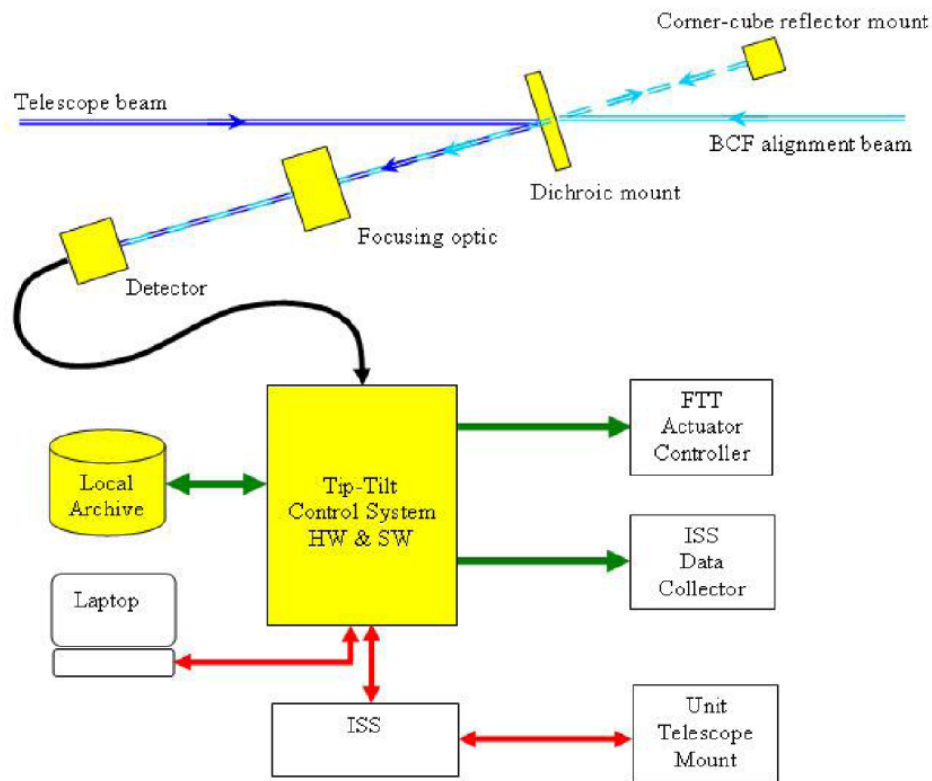


Figure 2: Block diagram of the FTT/NAS. The optical layout suggested is conceptual only: the actual layout, which is required to accommodate other systems installed on the Nasmyth optical table, is presented below.

The Andor EMCCD is only guaranteed to operate effectively at a temperature above 0 °C and in a non-condensing environment, and so the FTT/NAS camera will be enclosed and a thermal control system supplied to maintain the temperature and humidity inside the camera enclosure at all times. This system will extract heat from the enclosure and dump it to a chilled fluid loop in the UTE so as to prevent the camera overheating and to minimise heat dissipation to the air. These details are not apparent in Figure 2 which does not show any interfaces with the two fluid cooling loops available within the UTE.

Although it presents only a partial conceptual schematic of the FTT/NAS, Figure 2 reminds the reader that a critical design goal for the FTT/NAS is the need to ensure that its optics, together with the dichroic and the sensor camera must remain sufficiently stable in tilt and displacement such that the tip-tilt zero point does not move by more than roughly half a micron on the detector surface over a night's observations<sup>3</sup>.

To meet such high stability requirements we have chosen to use mounts without adjusters for the optical components: every component, once installed, will be fixed in position. This in turn will require the system to be tolerant of focus changes so that focus adjustment is only required seasonally. These stability requirements demand low sensitivity to thermal changes and so thermal gradients across the component mounts must be minimised. This has led us to adopt aluminium rather than stainless steel or invar (which is too expensive) for the mount material.

The software/electronic architecture of our proposed FTT/NAS implementation is covered in more detail in AD2, but it is perhaps useful to mention that our proposed design envisions the fast tip-tilt loop being closed in software rather than with additional hardware, e.g. reconfigurable electronics such as FPGAs. This approach

<sup>3</sup>The exact requirement given in RD1 is a variation of no more than 0.015 seconds of arc on the sky for a temperature change of 5 °C.

minimises the system’s electrical power consumption, since only a conventional rack-mount PC (with no additional FPGA boards) is needed to satisfy all the computing needs (including thermal management of the camera enclosure). Basing our system on a standard PC has also allowed us to make the most extensive possible use of software libraries provided by the camera vendor.

A fixed frame rate of 1 kHz will be used for all but the faintest targets (there is no noise penalty for this due to the on-chip amplification) but the closed-loop bandwidth will be user-selectable by means of adjustable servo parameters that allow the degree of time-averaging of the correction signal to be altered by the user/ISS. With this frame rate a latency of less than 790 microseconds is needed to meet the goal of a 50 Hz closed-loop bandwidth in fast tip-tilt mode (RD2): a somewhat larger value is allowed for the 40 Hz requirement. We have established that the Andor iXon X3 897 EMCCD can satisfy the derived requirements for a 40 Hz closed-loop bandwidth with a custom CCD clocking scheme using a  $32 \times 32$  pixel sub-frame. This sub-frame size will be sufficient, under worst-case conditions, to allow tip-tilt correction using an off-axis reference star for at least 300 seconds, before a brief ( $< 1$  second) interruption to fast tip-tilt mode is needed to reposition the sub-frame. No such interruptions are anticipated for the more common case of on-axis guiding, or when the field-rotation for an off-axis guide star is smaller.

A range of V-band magnitudes from 3.3 to 16 for the tip-tilt reference object can be accommodated by our design simply by switching between a high EMCCD gain setting ( $\sim 250$ ) and zero gain at an appropriate magnitude ( $\sim 8.5$ ). If brighter objects are required to be observed, a means of attenuating the signal (such as a pupil mask or neutral density filter) will need to be introduced. Currently we have not yet included this feature in our preliminary optical design, but we have no reason to believe this will be difficult.

## 4 Optical Design and Layout

### 4.1 Optical configuration and layout

Since the date of the CoDR we have frozen on a particular layout for the FTT/NAS optical train. This is shown in Figure 3. The essential features of this layout can be summarised as follows:

- Interception of the 95 mm diameter collimated output beam of the telescope with a large dichroic splitter. This diverts the “bluer” light to the FTT/NAS and allows the “redder” wavelengths to be transmitted to the Beam Combining Facility via the M4 mirror;
- Focusing of the collimated beam using a large diameter apochromatic lens. For this application we have traded-off the slight chromaticity of a lens-based solution with the much more demanding angular stability ( $\times 20$ ) and installation tolerance ( $\times 9$ ) needed for a non-chromatic off-axis parabola. We believe this design choice has been pivotal in us realizing a high level of stability for our implementation of the FTT/NAS;
- Folding of the converging beam path using two plane mirrors, so as to allow a long focal length for the camera lens to be accommodated on the rather compact Nasmyth optical table;
- Optimisation of the geometry of the folded path so as to keep the four principal optical components as close together as possible — these are all co-located on a single stiff baseplate — and so as to locate this baseplate and the sensor head and enclosure as far away from the table edge as possible.

The selection of this layout was in large part determined by a number of practical constraints on the space available on the Nasmyth optical table, which may not be evident from Figure 3. In particular possible layouts had to accommodate the following “boundary conditions”:

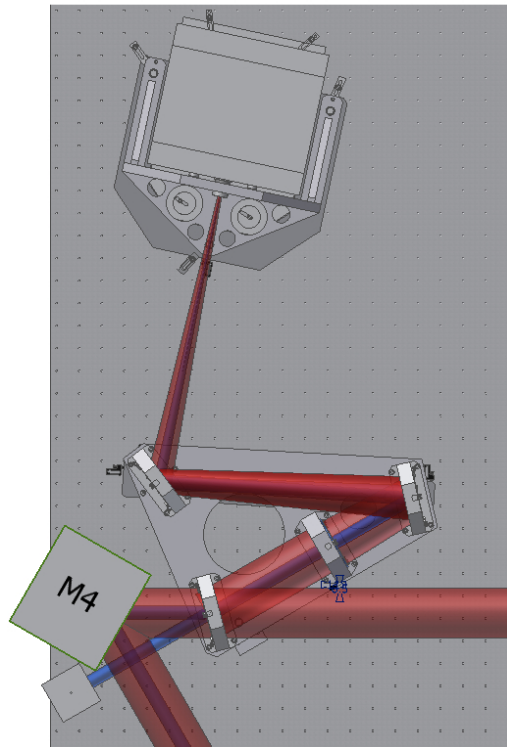


*Figure 3: A schematic diagram outlining the geometry of the FTT/NAS opto-mechanical layout. The beam from the UT tertiary mirror enters from bottom right and is intercepted by the dichroic to the right of the M4 mirror. The reflected beam passes through an apochromatic lens, and is focused onto the FTT/NAS camera sensor (at top) after reflection off two fold mirrors.*

1. The finite size and orientation of the UT Nasmyth table. Its short dimension running parallel to the direction of the exit beam from the telescope tertiary mirror has meant that all the layouts we investigated had to incorporate fold mirrors;
2. The presence of additional systems on the Nasmyth table, a number of which are not movable. Most of these are not visible in Figure 3, but they broadly speaking occupy the bottom right hand side of the figure, where space has been pre-allocated for a large ADC unit and a pick-off unit for an AO system, and the top right hand part of the figure where space has been reserved for an AO system and some smaller components of the Automated Alignment System of the interferometer. Some small variation of the locations of these units is allowed, but their footprint occupies roughly 50% of the half of the table closest to M3. One additional optical element of the AAS can be seen at the bottom left of the figure. This is a corner cube that is used to intercept the blue-coloured “pilot” beam that is sent back through the dichroic toward the FTT/NAS sensor for alignment purposes. There is very little scope for locating this component anywhere else on the optical table. This is also the case for the M4 mirror unit since it has to divert the outward-going beam towards a fixed aperture in the enclosure wall;
3. As well as these components present on the Nasmyth table, the UT and its enclosure also severely limit the space envelope available for the FTT/NAS. In particular, there is a hard limit to the maximum height that any element of the FTT/NAS may present above the table surface. This has had most impact on the possible locations for the sensor head, and how it can be packaged in its thermal enclosure;
4. A final degree of freedom that we have not been permitted to explore is the angular orientation of the dichroic mirror that serves to divert the bluer light to the FTT/NAS and transmit the interferometric beam. The interferometer system design has as a priority a requirement to allow the array to observe polarised

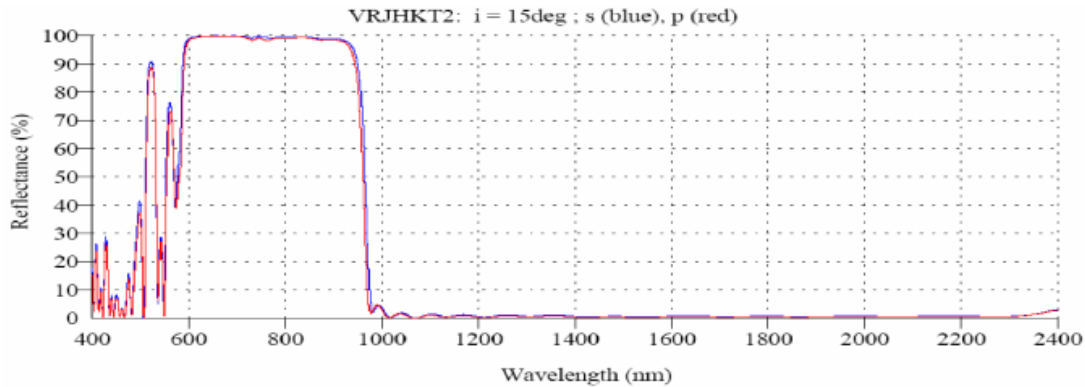


Figure 4: Predicted dichroic performance for the current design of the Phase I FTT/NAS dichroic. The red and blue curves refer to the two orthogonal linear polarisation states. Between 600 nm and 950 nm the mean reflectance is greater than 99%, while within the J, H and K near-infrared windows the transmission is greater than 99%. Experience with a previous, albeit less optimised design (mean reflectance approximately 96%), showed agreement between the measured and design performance at better than the 1% level over the full 600 nm to 2400 nm passband.

targets in total intensity, and so the global optical layout of the array and the optical coatings have all been designed for angles of incidence of either  $0^\circ$  or  $15^\circ$ . The impact of this for the FTT/NAS is that the angle between the beam hitting the dichroic mirror and that redirected towards the FTT/NAS sensor has had to be fixed at 30 degrees.

A rather different issue that we have had to deal with is the extent to which any initial layout for the FTT/NAS must support future expansion of the capabilities of the MROI. This has been accommodated in two ways. First, all the optical layouts that were considered were not allowed to encroach on the footprints of the AO and ADC systems even though these are not expected to be present for several years after first fringes have been detected. Second, all the layouts investigated were forced to leave space surrounding the dichroic mount to allow a larger mount handling two switchable components to be installed when a visible light interferometric instrument is installed. The design of such a mount is beyond the scope of this preliminary design, but we believe that we have been generous with our space allocation to allow this enhancement in Phase II of the MROI deployment with our proposed design.

## 4.2 Optical component choices

### 4.2.1 Dichroic

Our current optical system design utilises an Infrasil dichroic substrate of thickness 19 mm and diameter 127 mm. This has been procured with surfaces flat to  $\lambda/10$  PV (at 633 nm) and with its faces parallel to 5 minutes of arc<sup>4</sup>. At present we have not had this coated but, as was mentioned at the CoDR, we already have designs for both the Phase I and Phase II dichroics (see, e.g. Figure 4) and it only remains for us to optimise these for the specific material properties used by our selected vendor before we can have these fabricated.

As for the fold mirrors described below, the dichroic will be fabricated leaving a 6 mm uncoated annulus around its edge, so that the hard points on which it is mounted do not crack its dielectric coating. The one risk area we have yet to investigate is the longevity of the dichroic coating. Given that the FTT/NAS will inhabit a relatively

<sup>4</sup>Precise parallelism of the dichroic faces is not a design requirement since only changes in this quantity as a function of temperature will impact the zero-point stability of the system.

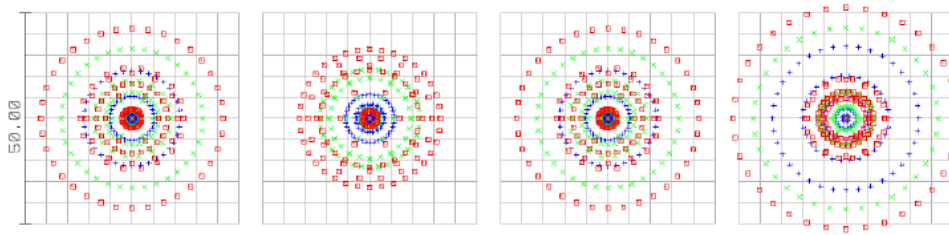


Figure 5: Polychromatic spot diagrams for a 1.5 m focal length cemented achromatic triplet comprising N-BAK4, N-KZFS4, and N-LAF2 elements. The blue, green and red symbols code for observing wavelengths of 400 nm, 600 nm, and 900 nm respectively. The spot diagrams are overlaid on a 5 micron pixel grid, so that the total extent of each panel is 50 microns  $\times$  50 microns. In all cases the 50% encircled energy diameter is less than 16 microns. The sequence from left to right corresponds to the ambient temperature changing from  $-5^{\circ}\text{C}$  to  $+10^{\circ}\text{C}$  in  $5^{\circ}\text{C}$  intervals. An expansion coefficient for the optical table surface of 17 microns/m/K has been assumed.

malign environment, it is likely that we will request that a lightweight cover be fitted over the FTT/NAS so as to limit the deposition of dust and moisture on its optics during its lifetime.

#### 4.2.2 Fold mirrors

The FTT/NAS fold mirrors will be fabricated on fused silica substrates, with identical dimensions to the dichroic substrate. The use of fused silica has been preferred since it has a CTE closer to Aluminium than Zerodur. These mirrors will be delivered with surfaces flat to  $\lambda/20$  PV (at 633 nm) so as to meet the top-level wavefront error budget for the MROI. Our current testing has been undertaken with mirrors with protected Aluminium coatings but we expect to deliver these COTS components with protected silver coatings giving a mean reflectivity between 400 nm and 1000 nm of approximately 95%.

#### 4.2.3 Focusing optic

We have chosen a custom 1.525 m focal length triplet lens to use as the focusing optic in the FTT/NAS, giving a focal plane scale of 9.175 milli-arcseconds per micron. This will have a clear aperture of 150 mm and comprise three cemented elements made of N-BAK4, N-KZFS4, and N-LAF2 glasses. These have been chosen so as to give excellent achromatic performance from 400 nm to 900 nm and a temperature-dependent focal length that will largely compensate for any thermal expansion/contraction of the steel top of the Nasmyth optical table (see, Figure 5). As a result, we do not expect to have to refocus the FTT/NAS during the night, though inter-seasonal focal changes may be necessary. We do not expect to realise these through the use of any actuated component, but rather, e.g., by utilising fixed exchangeable spacers.

We have discussed the design and fabrication of our custom triplet with a manufacturer, and after some adjustments associated with reducing manufacturing risks, we have been able to obtain an ROM cost for the optic consistent with our system cost budget. The only risk associated with its design appears to be the potentially long lead time needed to grind and finish the large elements. The design uses common, easily worked, glasses and according to our preferred supplier should be relatively straightforward to manufacture.

Currently, we have been using a simpler two-element COTS optic to test the prototype opto-mechanical hardware for the FTT/NAS. This has roughly the same dimensions and outer radii of curvature as the custom triplet, as well as a similar focal length, CTE and mass, so we are confident that our opto-mechanical tests satisfactorily mimic how the triplet will behave in the final lens mount.

### 4.3 Throughput

We expect the throughput of the optics for the FTT/NAS to be roughly  $0.98 \times 0.95 \times 0.95 \times 0.97 = 0.86$ . Here we have assumed 2% losses at the dichroic, 5% losses at each fold mirror and a 3% loss for transmissive losses at the lens. COTS broadband anti-reflection coatings typically deliver better than 99% transmission averaged over the 400 nm to 1000 nm bandpass, and so the major loss from the lens will be due to internal absorption.

These numbers are consistent with the sensitivity budget outlined in Sec. 2.8 above, and suggest that the selection of a transmissive, rather than all-reflective, optical layout is unlikely to have led to a non-optimal optical design from the point of view of limiting sensitivity.

## 5 Camera Selection

As has been mentioned above, our proposed implementation for the FTT/NAS will utilise an Andor iXon X3 897 EMCCD camera. The evaluation criteria used to arrive at this selection were presented in detail at the FTT/NAS Conceptual Design Review, and so are only mentioned briefly here. In short, this camera was able to meet all our derived requirements associated with cost, cabling, mechanical stability, and heat dissipation.

However, at the time of the CoDR there still remained an uncertainty associated with the ability for an arbitrarily located  $32 \times 32$  pixel sub-array to be read out and made available in memory on a timescale that would meet our latency requirements. Our discussions with Andor had suggested these could likely be met with a sub-array no greater than  $23 \times 23$  pixels in size. Since that time, we have been able to test this custom readout mode and have established that it is satisfactory from a timing perspective.

We are currently waiting to validate results obtained using a newer custom readout mode that will allow a  $32 \times 32$  pixel sub-frame to be read out almost as fast, but with somewhat lower pattern noise. Modelling of this readout mode, when coupled with timing measurements of the actual camera hardware, indicates that this newer scheme should comfortably meet our 40 Hz bandwidth requirement, but not quite meet our 50 Hz goal. We expect measurement data from the vendor to be made available to us in the next few weeks, and will be able to provide an update to the Project Office on a short timescale afterwards. We have every reason to expect this larger sub-array readout mode to be successful, in which case the tip-tilt field-of-view will be 4.7'' square (regardless of the sub-frame size, the full-frame acquisition field-of-view will be 75'' square).

Two other minor risks were mentioned at the time of the CoDR. These concerned the camera shape and the maximum supported cable length for the possible camera choices. Fortunately, neither of these are an issue for the Andor iXon X3 897 head.

## 6 Opto-Mechanical Design

### 6.1 Overall opto-mechanical architecture

The FTT-NAS opto-mechanical system will comprise two main assemblies; (i) a common base-plate assembly and (ii) the EMCCD camera and its thermal enclosure assembly. The layout of the two assemblies is shown in Figure 6 which also identifies the space envelopes of other assemblies on the Nasmyth optical table. Our design exploits the use of a single baseplate upon which the dichroic mirror, the focusing optic, and the two fold mirrors needed to feed the EMCCD camera will be co-mounted. The rationale for this is that it will mitigate, to first order, the effects of any local differential tilts or deformations in the Nasmyth table induced during the night due to changes in temperature. Such local disturbances would lead to differential movements and

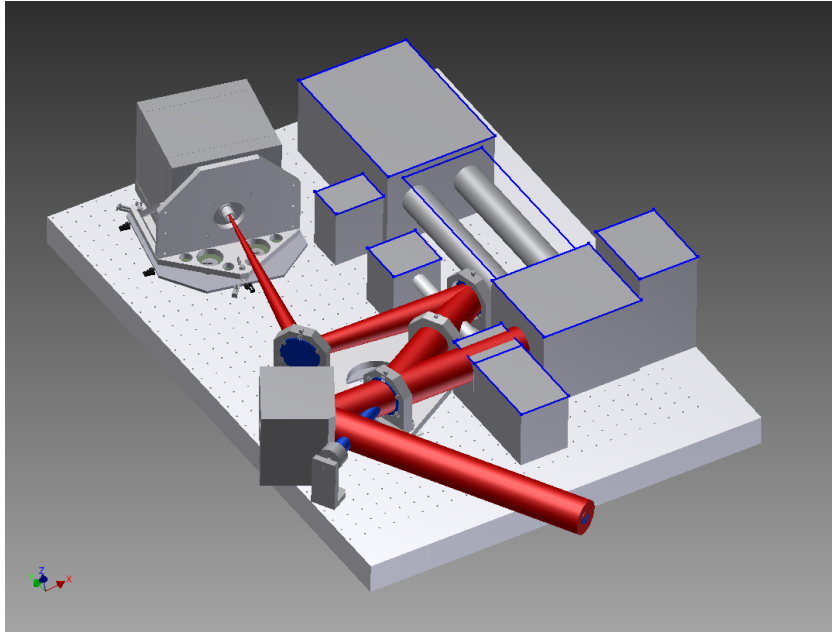


Figure 6: 3-d rendering of the FTT/NAS as it will be installed on the Nasmyth optical table. The grey boxes with blue boundaries represent the current space envelopes allocated to other hardware systems that will need to be located on the Nasmyth table. The beam from M3 is not shown, but enters from the right-hand side.

angular shifts of the FTT/NAS optical components and likely make the 0.015" zero-point stability requirement unrealisable.

The EMCCD camera will be mounted on its own baseplate which covers a significant area of the Nasmyth table so as to similarly reduce the effects of local deformations of the table surface during the night.

The common base-plate (including the optics mounts) and the EMCCD camera mount will be made of identical aluminium alloy and will both employ kinematic seat arrangements to allow for differential expansion of the base-plates and the steel of the optical table. The mounting components and materials of both assemblies will be matched to ensure that the centre of the focusing optic and the EMCCD camera move together as the temperature changes.

This common base-plate approach also allows all the optical components to be positioned accurately relative to each other so that the installation inaccuracies will be determined only by machining tolerances. These have been kept well within the allowed image quality misalignment budget. Although this design approach is able to minimise the effects of any deformation of the Nasmyth optical table due to temperature differences, the overall success of the FTT/NAS in meeting its zero-point stability goal will be fundamentally constrained by how stable the surface of the Nasmyth table is during the night. We believe the Project Office are aware of this, but remind the reader that the FTT/NAS stability budget only has to be met *on the assumption* that the Nasmyth table acts as a perfectly stable support.

## 6.2 Key sub-assemblies

### 6.2.1 Camera mount

The EMCCD camera mount assembly comprises five principal components:

1. The camera support structure;

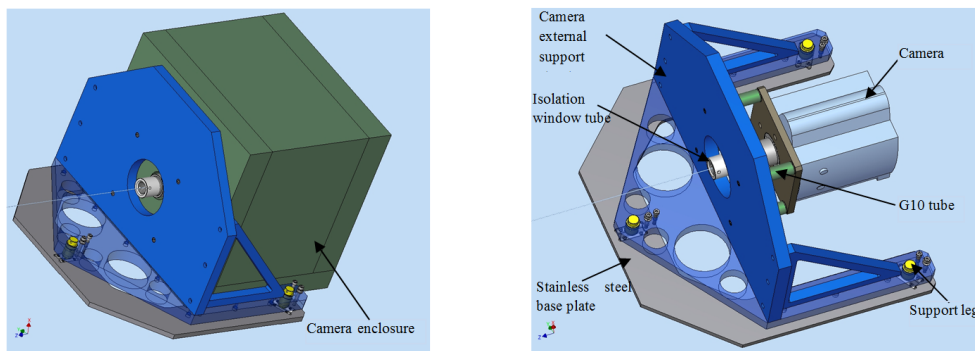


Figure 7: Two views of the FTT/NAS camera mount and thermal enclosure. In the left hand panel the base of the mount appears transparent to reveal the steel base-plate beneath. Two of the kinematic seats are visible together with their transit clamping screws. The tube containing window which isolates the air within the camera enclosure can be seen protruding from the central hole in the thermal enclosure and camera mount. In the right hand view, the thermal enclosure has been removed. The camera is mounted to a small interface plate which is connected to the external camera mount support structure via four thermally insulating tubes. The base of the support structure is shown transparent to reveal the U-shaped base-plate which is clamped to the optical table.

2. The mount structure and kinematic interface;
3. The base-plate and its kinematic seats;
4. The camera thermal enclosure;
5. An isolation window mount assembly.

An overview of the overall assembly is shown in the left hand panel of Figure 7. In our design the camera body is fixed to an aluminium interface plate which is connected to the mount structure using four thermally insulating tubes. The mount structure engages on the base-plate through a kinematic seat arrangement and the base-plate is clamped to the optical table. A thermal enclosure completely surrounds the camera but is supported independently from the optical table. This design allows the camera support structure to experience the same temperature as the opto-mechanics which relay the pick-off beam from the telescope yet allow the camera to be operated at a higher temperature environment. The pick-off beam passes through a thermal isolating tube and window to reach the camera detector window. This tube and the camera support tubes pass through holes in the front wall of the enclosure. A gap between the outer surfaces of the thermal enclosure and the mount structure minimises heat transfer from the enclosure to the mount.

The mount structure will be manufactured from the same material as the common base-plate optics mounts. In addition, the kinematic seating for both assemblies will make use of equivalent materials and height settings. Since the camera support structure experiences the same thermal environment as the common base-plate and optical component mounts, the change in height of the camera and the optical train due varying ambient temperature will be equal and thus will minimise any temperature induced drift of the tip-tilt zero point on the EMCCD.

**Camera support structure** The camera support structure revealed in the right hand panel of Figure 7 connects the camera to the mount structure (which is outside of the thermal enclosure) via stiff, low thermal conductivity tubes. The tubes are made from a glass fibre composite (type G10) with aluminium stubs glued to each end for mounting purposes. They provide an effective thermal break to prevent heat being transferred from the camera to the mount structure while maintaining good stiffness and dimensional stability.

**Camera mount structure** The mount structure consists of a large vertical plate, a horizontal U-shaped base and two triangular side frames. They are fixed together using screws to produce a solid structure from which the camera is cantilevered. This assembly seats kinematically on a large stainless steel base-plate which is clamped to the Nasmyth optical table. The mount structure will be made from the same low stress, aluminium material (aluminium MIC-6) as the FTT/NAS optical mounts and common base-plate.

**Base-plate assembly** The stainless steel base plate is fixed to surface of the Nasmyth table using a set of adjustable clamps. The base-plate will be manufactured from stainless-steel (grade 1.4003) which has a coefficient of thermal expansion very close to that of the skin material of the Nasmyth optical table and therefore no critical stresses are expected to be developed at the interface when the ambient temperature changes. To provide locations for the kinematic seats three pockets are accurately machined on the plate to accommodate three pairs of kinematic cylinders (see, Figure 8). The truncated cylinders (Bal-tec 312-TCR-CB), are mounted in the pockets via screws and the side walls of the pockets will provide their accurate positioning reference. The axes of these three seats i.e. a line running parallel to and mid-way between the bars intersects at a point directly beneath the camera focal plane. This will ensure that the camera sensor does not move laterally when the aluminium camera mount expands or contracts relative to the base-plate. The U shape geometry of the base plate provides space for accommodating the insulating base which supports the camera thermal enclosure cold plate assembly.

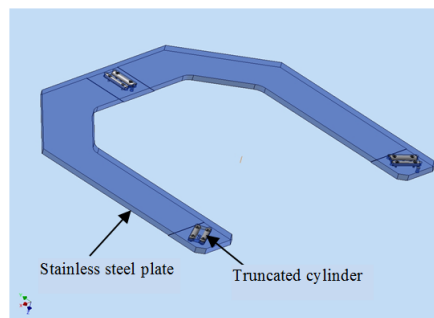


*Figure 8: The camera support base-plate will be a U-shaped stainless steel plate into which are set three kinematic seats each consisting of a pair of parallel cylinders. To preserve the camera lateral position with temperature changes, the central axes of these seats meet at a point directly beneath the camera sensor.*

**Kinematic interface assembly** The kinematic interface is aimed at minimising any stress and component deformation that would otherwise be caused by the different CTEs of the camera mount structure and the stainless steel base with changes in ambient temperature.

The design of the interface will be achieved using commercially available kinematic components. The camera mount structure is supported by three aluminium screws set into its base-plate at positions that coincide with the kinematic seats set into the steel base-plate. A truncated ball (Bal-tec 50TBR) is glued on the end of each screw using epoxy. The height and tilt of the camera can be adjusted via turning the threaded screws and then applying an aluminium locking screw. To protect the kinematic interfaces during the transport of the telescope, the balls and the cylinders can be separated by lifting up the camera mount structure using a set screw (M5 screw 1) and then clamping at this position using M5 screw 2 which incorporates a spring to provide a safe preload.

**Isolation window assembly** An isolation window will be needed to separate the warmer air within the camera enclosure from the outside air. To provide for this, an acetal barrel assembly (see, Figure 10) is mounted on the camera support structure and protrudes through the thermal enclosure insulation and a hole in the camera

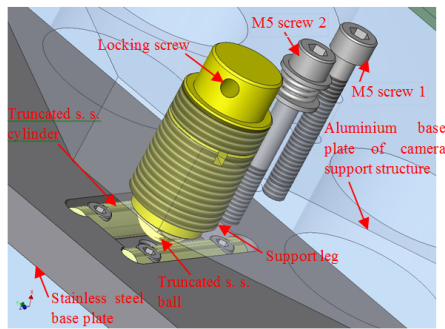


Figure 9: Each kinematic support consists of a support leg or screw set into the camera mount base. The screw has a ball end which impinges on the two cylinders of the kinematic seat set into the steel base-plate. A locking screw is applied when the correct height setting is achieved. Two M5 screws allow the interface to be locked in a separated position when the telescope is transported.

mount structure. The barrel consists of two tube sections: a removable front section and a rear section which will be fixed to the camera support structure. A 25 mm outer diameter window is mounted on the front section via a retaining ring. The front tube section is screwed onto the rear tube section and extends sufficiently beyond the camera mount so that it is easy to remove for window replacement. The inside of the tube will be machined with fine pitch grooves to diminish stray light reflections. The isolation window is positioned within the tube coincident with the outer surface of the enclosure insulation. This design allows replacement of the window with another of the same diameter and similar thickness and consequently it can also act as a filter for the FLC.

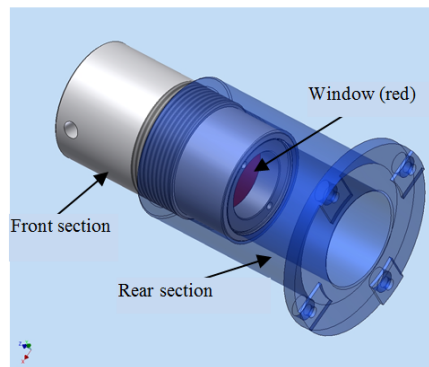
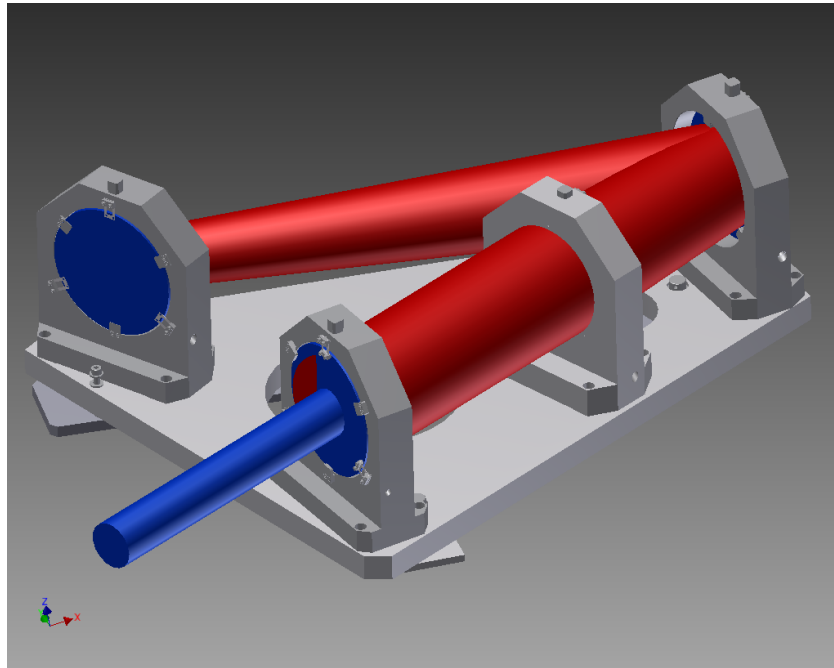


Figure 10: The isolation window assembly consists of two tubes. The rear section is fixed to the camera interface plate and the front section unscrews from outside the thermal enclosure to allow the central window (or filter) to be replaced.

### 6.2.2 Optics baseplate

This assembly supports all the optical components of the FTT/NAS imaging system, i.e. the dichroic, the focusing optic and two relay mirrors to fold the beam on its path to the FTT/NAS camera. The base-plate complete with optics and mounts is shown in Figure 11. The purpose of the base-plate and its associated optics is to split off some proportion of the science beam from the telescope and focus it onto the FTT/NAS camera and remain inherently stable so that any that movement of the image on the camera is not the result of changes of the optical arrangement due to changes in ambient temperature.

The optic mounts (which have recessed bases) will be bolted to the base-plate, at each of four locations. The



*Figure 11: The common base-plate complete with optical components in their mounts. The beam path is illustrated in red. The nearest component is the dichroic. Light (not shown) from the telescope enters from the right and a portion (shown in red) is reflected to the focusing lens and then onto the first fold mirror and back to the second fold mirror (at left). From there the beam is directed onto the FTT/NAS camera (not shown).*

base-plate is supported on three kinematic seats in the classic cone, vee and flat arrangement that allows the aluminium plate to expand or contract with respect to the Nasmyth optical table without change of orientation. This ensures that all the angles in the optical system are maintained as temperature changes affect the base-plate and the Nasmyth table which have significantly different CTEs. These kinematic seats, two of which are partially visible underneath the base-plate, are made of steel with a CTE very close to that of the optical table and clamped to the table so that the base-plate can be positioned with precision in the correct orientation with respect to the incoming light beams and the FTT/NAS camera.

The base-plate will be made from aluminium MIC-6 (a low stress grade) as will the optics mounts. It will be 25 mm thick and have two light-weighting holes. There are three height-adjustable kinematic ball studs, one situated near each corner of the base plate. The top of one of these is visible near the first fold mirror, another is situated under the dichroic mount and the third is situated directly under the second fold mirror mount. Each ball locates into a unique kinematic seat clamped to the surface of the Nasmyth table. The seat underneath the second fold mirror is conical and thus locates the ball precisely at a point in the x-y plane of the table-top. The seat near to the first fold mirror is formed from two precision parallel steel bars which locate the associated ball in the direction transverse to the axis of the bars, hence determining the orientation of the base-plate in the horizontal plane, but allowing sliding of the ball along the bars. The third seat, near the dichroic is a precision flat plate. This will allow the associated ball to translate in any direction without change in height.

This kinematic seat arrangement is shown in Figure 12. There are two key parts to this interface: the long strip carries the cone seat and the parallel bar seat, while the individual seat is the precision flat plate. The cone and parallel bar seats are mounted on one strip because it is important that the bars are parallel with a line between the centre of the cone and the centreline between the bars. This will ensure that there is no rotation of the base-plate about the cone in the horizontal plane as the ball slides along the bars when the temperature is changing. The centre of the ball associated with the cone seat is coincident with the plane defined by the reflecting surface of the flat mirror in the mount directly above. This ensures that, as the base-plate expands and contracts with

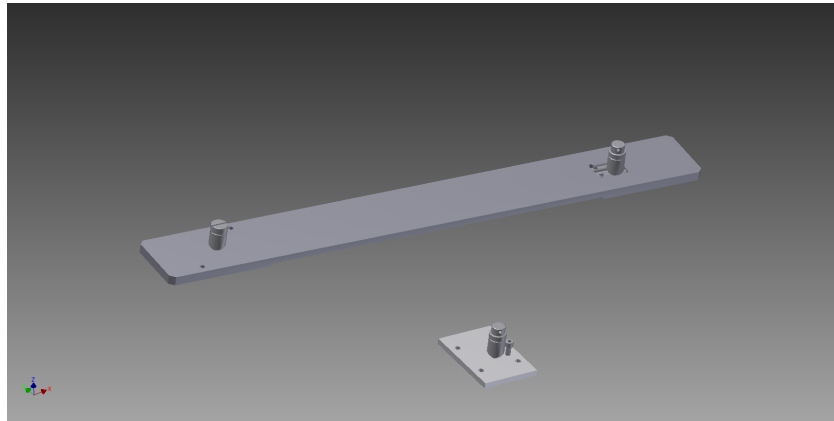


Figure 12: The kinematic seat arrangement showing the cone and parallel bar seats mounted on one strip while the flat seat is a separate component.

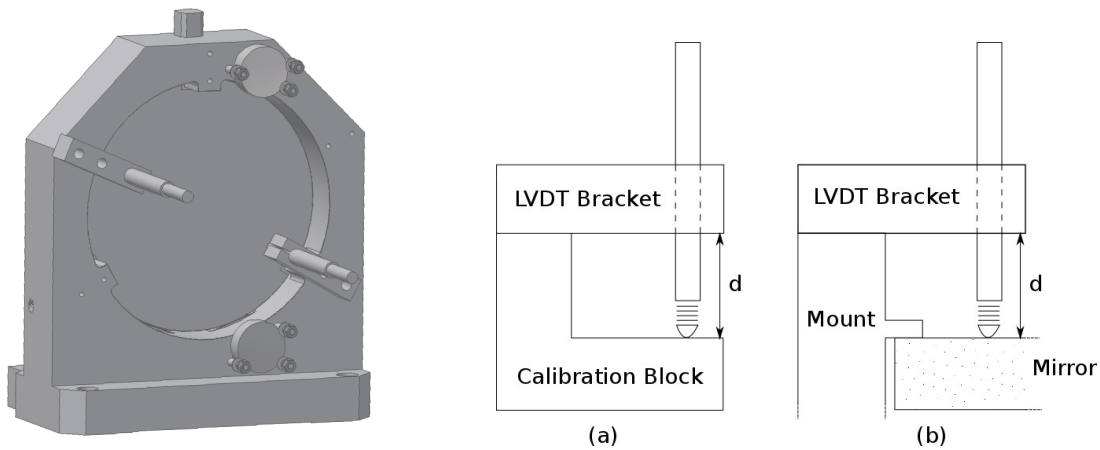


Figure 13: A 3-d view of the dichroic/fold mirror mount with two LVDT probes attached (used for testing purposes). These directly measure the distance to the surface of the mounted optic from the LVDT bracket fixtures. The two right hand panels show the method by which the probes and their mounting fixtures were calibrated by measurement of an aluminium calibration block that had the same material properties and dimensions as the dichroic/fold mirror mount (see Sec. 10 for details).

respect to the Nasmyth table the point of intersection of the incident light beam passing through on its way to the camera does not move with respect to the Nasmyth table to which the camera is also fixed nearby.

### 6.2.3 Dichroic & fold mirror mounts

The current dichroic/fold mirror mount design is shown schematically in Figure 13. This is a monolithic symmetric aluminium component in which the front reflective surface of the optic (either the dichroic or a fold mirror) is sprung loaded onto three symmetrically disposed hard points. These define the orientation of the reflecting surface in the x- and y-directions, i.e. perpendicular to the beam propagation direction. The optic is supported at its base on two plastic rods and is lightly sprung loaded from the top so as to restrain it from moving in the vertical direction: the associated spring plunger can be seen at the very top of the mount in the half hand panel of the figure.

In the presence of temperature changes the whole of the mount is designed to expand about its center. The

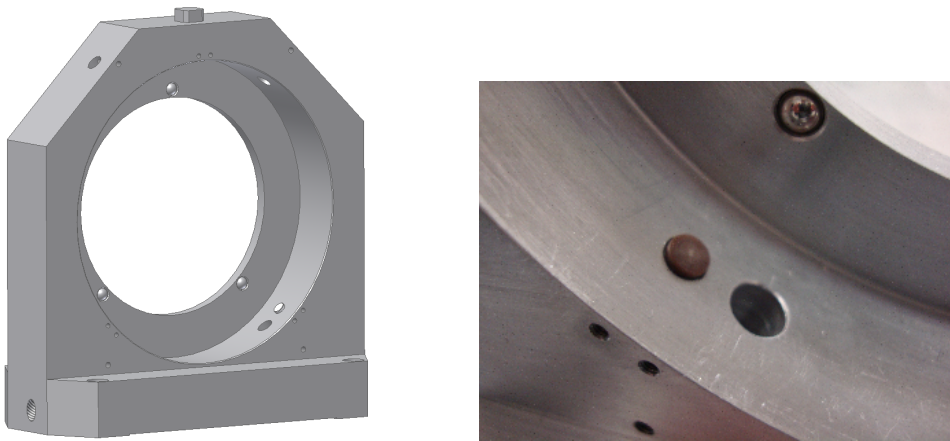


*Figure 14: A 3-d view of the triplet lens mount. The detail at right shows one of the spherical hard points (at top) as well as one of the plastic support rods. The additional empty hole next to the support rod allows LVDT probes to be inserted such that they can measure the shear of the lens once it is installed in the mount. The pair of holes near the edge of the front face is where one flat spring attaches.*

mount has the optical hard points located in the central plane of the mount so that as the mount expands and contracts, the angle of the optic should not change. Furthermore, even in the presence of a top-to-bottom thermal gradient (the most likely expected on site) the mount is designed to preserve the orientation of the optics.

#### **6.2.4 Lens mount**

Our proposed lens mount is shown schematically in Figure 14. This is similar to the dichroic/fold mirror mount in that it is a monolithic symmetric aluminium component. The lens is supported by three plastic rods around its edge, and its front surface is pushed onto three hard-points from behind by three flat springs. In this case, due to the curved front surface of the lens, the hard points are not flats, but balls set into the mount. One of these can be seen in the detail shown in the right hand panel of figure 14.

The plastic supporting rods have been chosen so that in the presence of temperature changes these will expand/contract in such a way that the combination of the CTE of these polymer pins and the lens glass will exactly mimic the expansion of a solid block of aluminium, or equivalently the aluminium camera mount. This “material compensation” allows for the differential motion between the mount and the lens to be corrected if the length of the polymer pins is suitably chosen. This thereby maintains the position of the vertex of the lens at the centre of the mount’s clear aperture independent of temperature.

### **6.3 Mass budget**

The total mass of the common base-plate assembly is approximately 26.7 kg, including all of the optics and mounts, and the kinematic seats that clamp to the optical table. The total mass of the EMCCD camera assembly, including mount, base and thermal enclosure is approximately 30.6 kg. The allowance for all FTT/NAS components in the mass budget provided in RD6 is 30 kg (10 kg for the dichroic assembly and 20 kg for everything else). Hence our design is over budget by approximately 27.3 kg. It is unlikely that the mass can be reduced much without affecting the opto-mechanical stability of the FTT/NAS.

The implication of this excess mass is that the Nasmyth optical table will have a slightly lower resonant frequency (assuming that the adaptive optics unit of mass 50 kg was fitted) than might otherwise have been

expected. Without the AO unit, the total mass on the table will be less than budgeted by 22.7 kg.

## 7 Thermal Design

The vendor-specified minimum guaranteed operating temperature for the FTT/NAS camera is 0 °C in a non-condensing environment and its minimum survival temperature is –25 °C. Therefore for operational and camera safety reasons the FTT/NAS camera will be located within an enclosure in which the air will be maintained close to ambient temperature but in any case not less than 0 °C. To prevent overheating of the camera, and to meet the maximum surface temperature constraints for hardware that is located near the optical beam, the camera enclosure will be insulated and heat removed from it.

Since the CoDR, we have adjusted the parameters of the thermal management strategy for the FTT/NAS in three minor ways:

- The camera enclosure insulation thickness has increased from 40 mm to 50 mm;
- The available cooling fluid flow has been confirmed to be at up to 3.6 litres per minute;
- The electronics cabinet cooling water loop has been chosen for use as the heat sink for the system.

These changes will improve the capability of the enclosure design to meet the enclosure residual heat allowance. Component tests conducted with a thermal chamber using a similar arrangement of cold plates have indicated that the cooling efficiency is likely to be better than predicted but this has yet to be confirmed using the camera in the enclosure design. The preferred coolant tubing used in the cold plate design is nylon rather than copper and a comparative test will be made to confirm the choice.

Our decision to use the electronics cabinet cooling loop has considerably simplified the control of the thermal system. There will be no need for any subsidiary cooling loop, pump and heat exchanger. This solution has the distinct advantage that the fluid that passes through the cold plates and then through the camera to remove the Peltier heat should never fall below 0 °C in normal operation. Consequently, there will be no need for a variable coolant flow through the camera enclosure. The desired flow will be set by a manually adjusted valve and monitored by a flow meter for safety and setting purposes.

### 7.1 Thermal enclosure design

The camera enclosure has been designed so that it completely surrounds the camera but does not rely on the camera mount for support, i.e. it is supported independently from the optical table. Details of the camera mount are given in Sec. 6.2.1 and the enclosure is shown in the left hand panel of Figure 7. The enclosure will be constructed from rigid thermal insulation panels bonded to the outside of an aluminium frame formed from the cold plates used to remove heat from the enclosure. The outer surface of the insulation panels will be covered with a protective skin of aluminium and the whole assembly will be supported from the optical table by low thermal conductivity spacers attached to the cold plate framework.

The cold plates are purpose designed and built so that the number of fluid connections within the enclosure is minimised. There will be three plates connected together to form an inverted 'U' shape. Each plate will be machined with straight channels to receive a nylon cooling tube which snakes to and fro so that the tube bends are outboard of the plate. Heat-sinks will be connected to the plates to hold the tubing in place and force a good thermal connection to the cold plate. Using this method a single run of tubing can be used for the whole cold plate system and the only connections will be those that are necessarily made to the camera. The tubing will be arranged so that the cooling fluid enters the enclosure, passes first through the cold plates and then through the camera before exiting the enclosure again.

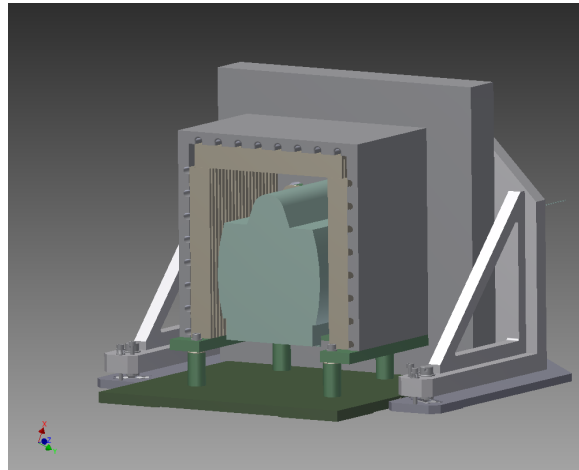


*Figure 15: View of the FTT/NAS camera enclosure with the insulation panels removed. The overall size of the enclosure is 340 mm tall by 340 mm wide and 320 mm deep and has insulation panel thickness of 50 mm. The camera is surrounded on three sides by finned cold plates which are connected in series with the camera Peltier cooling connections. The loops of the cold pipes running through the cold plates are shown in section. The camera is mounted to a bracket outside the enclosure.*

As can be seen in Figure 15, the cold-plate assembly will be mounted on a frame supported by four pillars bonded to a base-plate which is clamped to the table top. The frame, pillars and base-plate will be made from a special low thermal conductivity glass fibre composite and provide an effective thermal break. The overall dimensions of the enclosure will be approximately 356 mm high (including a 10 mm high thermal break to space the body of the enclosure from the Nasmyth optical table) by 340 mm wide by 320 mm deep. The insulation will be made from polyisocyanurate sandwiched between aluminium foil resulting in a thermal conductivity of 0.023 W/mK. A thickness of 50 mm will be used on all sides except the base which will utilise a thickness of 40 mm.

The camera will be located inside the enclosure on a mounting plate supported by pillars of low thermal conductivity glass fibre composite that pass through the insulation to the camera mounting bracket outside. A tube fixed to the camera mounting plate will also pass through the insulation and on through a hole in the camera mount. Mounted within the tube will be a window so that air within the camera enclosure is prevented from escaping. This window will also serve as a filter to enable guiding over an appropriate waveband and will therefore be exchangeable by unscrewing the tube externally. Thus the camera will be fixed only to the camera mount and will not be in contact with the enclosure which is to be supported independently from the optical table. This will reduce the influence on the camera of any forces acting on its enclosure.

A dry air supply will be connected to the enclosure to ensure that humidity levels are low. Thermal sensors will monitor the cold plate and enclosure air temperature and a humidity sensor will sense the enclosure air. A small heating element will be mounted in the enclosure so that the internal temperature can be increased if it is too cold for the camera to be operated. Also fitted to the outside of the enclosure, for monitoring purposes, will be a surface temperature sensor and an air temperature sensor.

The rear face of the enclosure will be removable for access to the camera electrical and fluid connections and to internal sensors and the protective thermal heater. With the exception of the camera cable all fluid and electrical connections will be terminated on an interface plate close to the camera enclosure.

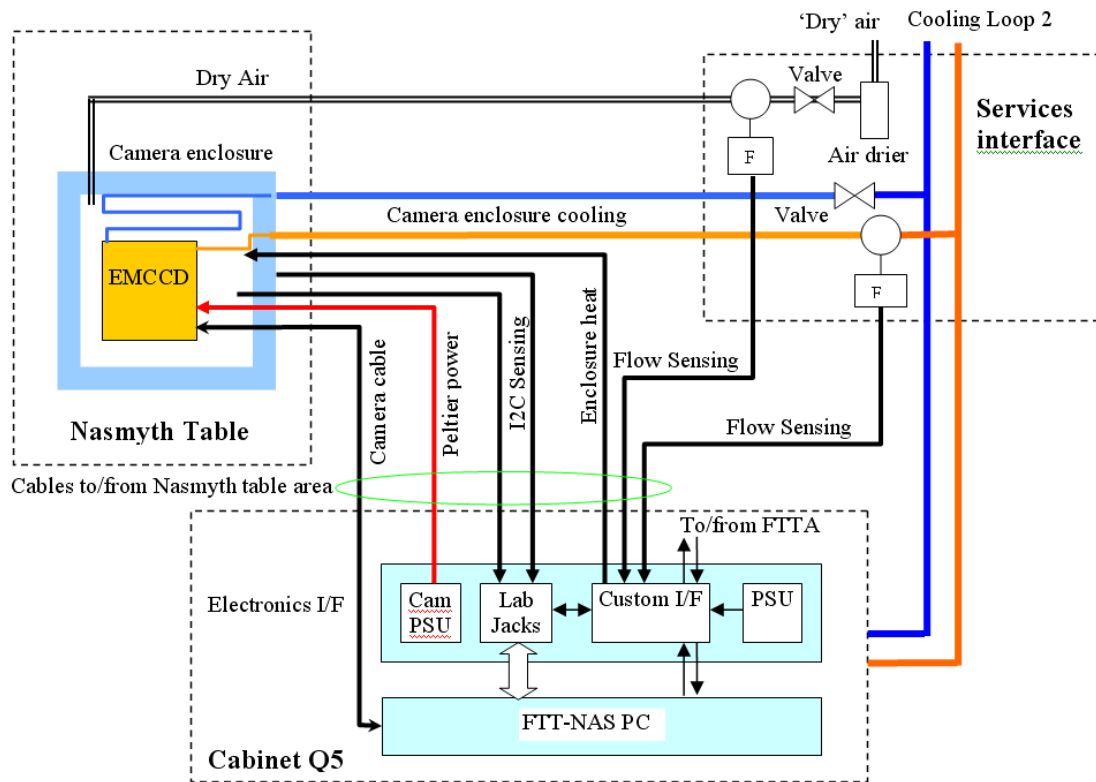


Figure 16: The FTT/FLC camera environmental control and monitoring scheme showing the connections between the camera enclosure located on the Nasmyth table, the services interface panel located close by, and the electronics interface located with the FTT-NAS PC in the telescope enclosure cabinet Q5. Connections to/from the FTTA controller, also located in Q5, are shown passing through the custom interface.

## 8 Electronics Design

The electronics for the FTT/NAS is located in the 5U of electronics space allocated in cabinet Q5 within the telescope enclosure. Of this space, 3U is allocated to the FTT/NAS PC and the remaining space is reserved for a 2U chassis which will accommodate the following electronics and modules:

- The EMCCD Peltier power supply module;
- Two Labjack analogue/digital I/O modules;
- A custom electronics interface circuit board;
- A power supply for the custom electronics.

The electronics design is concerned mostly with interfacing the signals between the FTT/NAS PC and the FTTA controller but also with providing analogue inputs for the various sensors that are necessary to monitor the camera thermal enclosure and the services provided to it. A diagram of how the FTT/NAS electronics in cabinet Q5 is interconnected with the camera and its services is shown in Figure 16. Descriptions of the PC, electronics interface and the sensing and services are presented in the following sub-sections.

## 8.1 PC and electronics interface

The FTT/NAS or FLC system software will run on a 3U rack mounted Intel-style computer which incorporates two special PCI cards: the camera interface and the interface to the FTTA controller. The candidate computer is an Amplicon Ventrax 2008-P4.1. The camera interface card will be the Andor CCI-23 that specifically interfaces with the EMCCD camera and which also supplies the power to the camera electronics. The candidate analogue interface to the FTTA controller for actuation of the fast tip-tilt mirror and monitoring of its current state is an Advantech PCI-1716/L.

Some signal conditioning of the high bandwidth analog signals to and from this card may be required and will be incorporated on the custom analogue interface board.

For sensing and control low bandwidth interfacing will be handled using two of the computer's USB ports. Each port will connect with a Labjack U3 to provide access to an I<sup>2</sup>C bus and a variety of digital and analog input and output connections. One bus will handle a humidity sensor and three temperature sensors associated with the camera thermal enclosure and the other bus will handle sensors placed outside the enclosure and on the Nasmyth table. The analog inputs available on the Labjack modules will connect via signal conditioning electronics on the custom circuit board to flow rate sensors used for monitoring the camera thermal enclosure coolant and dry air supplies. An analog output will control the camera thermal enclosure heater via an amplifier mounted on the custom circuit board. These interfaces do not have hard real time requirements and will run in Linux using libraries supplied by Labjack.

The sensing elements and control for the camera thermal enclosure will be:

1. The camera case external temperature sensor – for monitoring;
2. The camera enclosure air temperature sensor – for monitoring and control;
3. The cold plate temperature sensor – for monitoring;
4. A humidity sensor – for monitoring and control;
5. A heating element – for temperature control;

The heating element will be a power resistor fixed to the base insulation and driven by a voltage controlled DC current source on the custom electronics board.

The sensed elements outside the camera thermal enclosure will be:

1. The Nasmyth optical table temperature (in the vicinity of camera);
2. The temperature of common base-plate – for monitoring;
3. The air temperature above optical table – for monitoring;
4. A humidity sensor – for monitoring

The sensing elements associated with the services panel will be:

1. A coolant flow rate sensor – for monitoring;
2. A dry air flow rate sensor – for monitoring;

These flow sensors will be analogue types giving a DC voltage which is proportional to flow.

## 8.2 Services interface

The services interface will consist of a panel which is located on the Telescope Enclosure wall close to the Nasmyth table and below the camera. The enclosure services, i.e. the electronics cabinet cooling “cooling loop 2” and nominally dry compressed air from the enclosure air receiver will be brought to this panel where they will be interfaced to the connections from the camera.

The compressed air from the enclosure services will be passed through an air drier as an added precaution. The dry air will be passed through a manual set valve to adjust the flow, a flow sensor for monitoring purposes, and then to a self-sealing connector on an interface plate attached to the Nasmyth table close to the camera enclosure. A tube from the camera enclosure will connect at this plate. The preferred air drier is to be a low maintenance membrane type provided the base purge rate is not unduly high.

The cooling loop may terminate on this panel or continue to the cabinets, depending on how the piping is arranged. The cold feed of the cooling loop passes through a manual set valve (TBC) so as to provide a suitable flow rate for the camera enclosure. The flow rate available is 3.6 litres per minute so a set valve may not be necessary. An insulated pipe will link from the valve (if fitted) to a self-sealing connector on the interface plate on the Nasmyth table. An insulated pipe carrying the “warmer” return flow from the camera will run back to the services interface panel where it will pass through a flow sensor before reconnecting to the cabinet cooling loop. This arrangement ensures that any measured coolant flow has passed through the camera enclosure. Flying tubes from the camera enclosure will connect to the interface plate using self-sealing connectors.

Electrical connections from sensors in the camera enclosure, from the Nasmyth table and from the services panel will also be brought to the interface plate where they terminate with suitable connectors. Cables from the interface plate will run back to the electronics interface for the FTT system in Cabinet Q5. Only the special camera cable will run directly from the EMCCD camera within the camera enclosure to the PC located in cabinet Q5.

These arrangements will allow the camera enclosure, complete with camera (once the camera cable is unplugged), to be removed from the Nasmyth table.

## 9 Software Execution Environment

The software design for the FTT/NAS is described in detail elsewhere in AD2. Here we present a very brief overview of the environment in which this software will be run.

The software execution environment for the FTT/NAS is illustrated in Figure 17.

The system software will run on a rack mounted Intel-style computer. The currently preferred candidate computer is an Amplicon Ventrax 2008-P4.1. The operating system is expected to be Linux 2.6.32 with Xenomai 2.6 kernel patches, but the source code is compatible with more recent releases, including the forthcoming Xenomai 3.

Besides the interfaces to the FTTA controller and environment sensors described above, the computer will have a Gigabit Ethernet connection to the MROI control room via a local switch. This Ethernet link will be the conduit for the interface with the Interferometer Supervisory System and operator GUIs.

## 10 Testing Status and Results

The principal aspects of the FTT/NAS that have been tested experimentally to date are those related to camera performance, i.e. latency and functionality of readout, and opto-mechanical stability. The following sub-

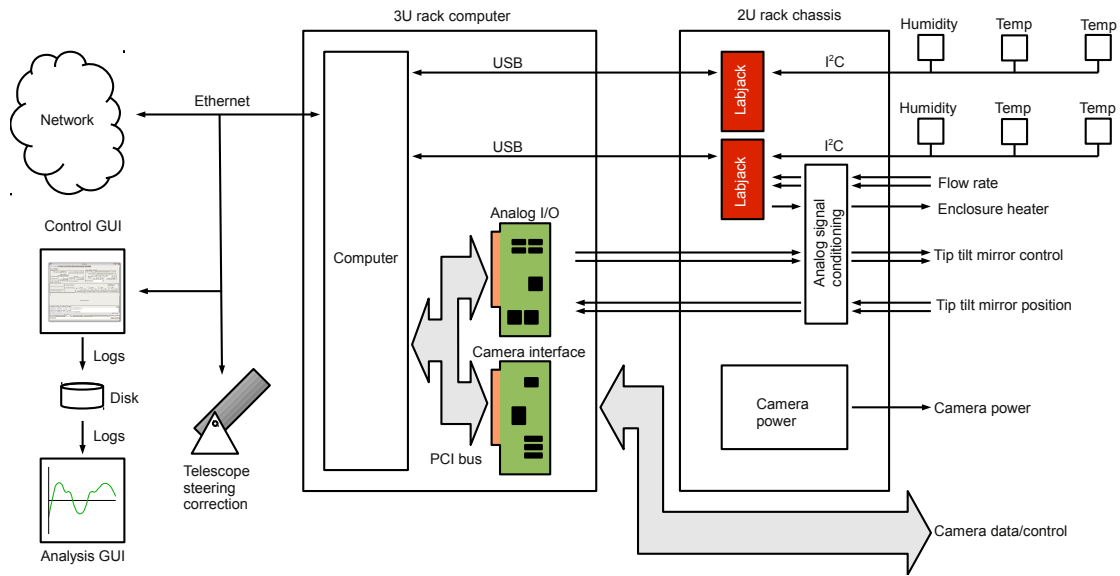


Figure 17: The proposed software execution environment for the FTT/NAS. Further details are provided in the main text and also in AD2.

sections outline these test procedures and results.

### 10.1 Camera readout testing

As described in Sec. 5 tests have already been undertaken with an initial  $23 \times 23$  pixel sub-array custom readout provided by the EMCCD vendor. These were reported in summer 2011 and confirmed that the frame rate and latency requirements for the FTT/NAS could be met with this small sub-frame with the camera operating at high gain and with an effective readout noise of  $\sim 0.25e^-$ .

Since then Andor have been customising a larger ( $32 \times 32$  pixel) sub-array fast-readout mode for us, and as of the date of this report (30th April 2012) they have confirmed that a 1 kHz frame rate is achievable. They have not yet reported any latency measurements to us, but using our own scope timings obtained with the smaller  $23 \times 23$  sub-array readout, we believe their latest fast-readout mode will deliver a closed loop bandwidth of just over 43 Hz. This meets our requirement, but not our goal of 50 Hz.

### 10.2 Opto-mechanical testing

Our opto-mechanical testing, which was reviewed most recently in December 2011, is described in more detail below. The first stage of our testing focused on assessing to what extent our proposed optical component mounts were able to meet the stability requirements needed for the FTT/NAS in the presence of the temperature changes expected at the Magdalena Ridge. More recently we have been testing the overall optical stability of the full optical system in a so-called “integrated test”. This latter testing is not fully complete and so only preliminary results are presented here. However, we expect to be able to update the Project Office on these results at the PDR and confirm in quantitative terms how well the prototype FTT/NAS meets its zero-point stability test under realistic environmental conditions.

### 10.2.1 Individual component testing

In order to test the thermal stability of the individual FTT/NAS component mounts, a thermal enclosure was constructed within which each of the mounts (with the relevant optic attached) could be introduced. The chamber was constructed of six cold plates, placed in pairs on the top and two side faces, which in conjunction with an aluminium baseplate made up a short tubular shell. The cold plates were supplied with temperature-controlled water from a Grant RC350G chiller, which was placed in an adjacent laboratory, and could be used to either warm up or cool down the chamber. The fluid temperature could be controlled to roughly one degree Celsius, which proved more than adequate for our tests.

By cycling the water temperature according to a pre-determined schedule, the optical component mounts could be subjected to “environmental” temperature changes mimicking those that might occur during an observing night. This method of testing, however, is likely to have introduced errors associated with non-uniform cooling/warming of the mounts due to the forced air circulation in the chamber (small fans were used) and possible uneven mixing of air in the chamber. These inaccuracies are most likely to have occurred at the start of each cooling cycle, as aggressive cooling of the chamber was taking place.

The optical mounts were typically set up within the chamber with position sensors attached such that any relative motion between the mount and the optic could be determined<sup>5</sup>. In addition, additional sensors were used to monitor, for example, the chamber temperature, the temperatures of different parts of each mount and the ambient temperature outside the chamber.

The position sensors used were Linear Variable Displacement Transducers (LVDTs) which were typically able to measure displacements as small as 50 nm. Because LVDTs themselves exhibit a temperature-dependent response, in all cases the measurements obtained with them were calibrated against known temperature dependent motions made with identical sensor/mounting arrangements. An example of this can be seen in Figure 13 which shows (at left) the dichroic/fold mirror mount with two LVDT probes mounted and touching the mirror surface, and (at right) two cartoons showing how the probes were calibrated by comparing the change in distance measured between their mounting brackets and an aluminium calibration block to that measured with the aluminium mount and its attached mirror.

**Mirror piston tests** A typical set of test results associated with the piston stability of the dichroic/fold mirror mounts, i.e. the extent to which changes in temperature give rise to motion along the beam propagation (z-) direction, is presented in Figure 18. This shows the uncalibrated z-motion of a fused silica mirror as a function of chamber temperature, in this case changing from roughly 13 °C to 23 °C, together with the uncalibrated measurement of a reference block. Also shown is the difference in these two measurements: this represents the actual calibrated piston motion of the optic. This is very stable with temperature, with only small variations of at most 100 nm peak-to-peak. This can be compared with a piston stability requirement of roughly half a micron, i.e. a factor of five larger, and confirms that the mounts are behaving as designed, easily meeting the FTT/NAS piston stability requirement.

**Mirror tilt tests** A typical set of test results associated with the tilt stability of the dichroic/fold mirror mounts is presented in Figure 19. In this case the left hand panel shows the uncalibrated LVDT data in blue, the LVDT calibration data in red, and the difference of these two, representing the actual tilt, in black. The graph has been scaled such that a linear displacement of 0.045 microns corresponds to the stability requirement for the dichroic mirror mount (i.e. 45 milliarcseconds).

The data appear to show a slowly decreasing trend with temperature (this is again rising by roughly 10 °C over the course of the ten-hour measurement time) of about 0.075 microns, i.e. roughly 70% greater than

---

<sup>5</sup>An earlier strategy that involved optical sensing of any component movements proved unsuccessful, as it proved too difficult to control the turbulence through the paths along which the probe optical beams were propagating.

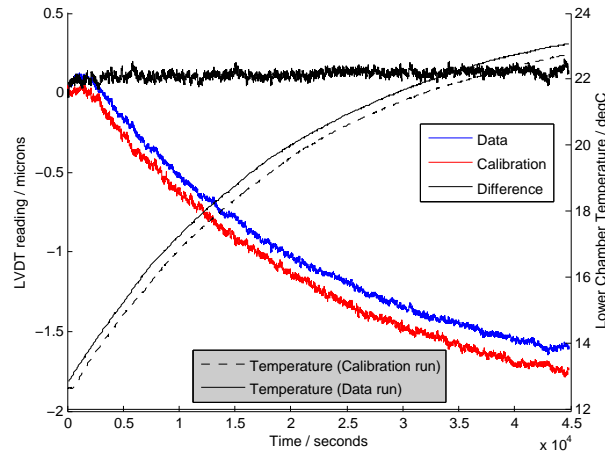


Figure 18: Raw (blue and red) and calibrated (black) piston fluctuations measured in a typical dichroic/fold-mirror piston test. There is a small (quarter of a degree) difference in the temperature profile for the measurement and calibration experiments, with the temperature in the test chamber rising from roughly 13 °C to 23 °C in each case. Note that the raw uncalibrated measurements only show a variation at the micron level, i.e. only a factor of a few greater than the allowed piston fluctuations.

the FTT/NAS budget allows. In order to assess the reliability of this result, additional experiments were run where calibration data from a given experiment were calibrated using measurements from a calibration made on a different day. One such "cross-calibrated" dataset is shown in the right-hand panel of Figure 19. In this example the colored lines again show the behaviour of the uncalibrated measurements, while the black trace represents the best estimate of the calibrated angular tilt. These data suggest that our test set-up is limited by calibration uncertainties to a level of no better than twice the angular shift allowed by the optical stability error budget.

In itself this is disappointing from the point of view of our testing strategy, but on the positive side all our experimental data suggest that the dichroic/fold mirror mounts are unlikely to have exceeded the tilt stability budget allocation by any more than a factor of two.

**Lens shear tests** The tolerances on the tilt and piston stability of the FTT/NAS lens mount are factors of 10–100 times greater than for the dichroic/fold-mirror mounts, and so given that they share a common design approach, tests of these aspects of the lens mount stability have not been prioritised. Rather, it is the stability in x- and y-position of the lens, perpendicular to the direction of beam propagation, that is likely to present the greatest design challenge. Table 3 makes clear that the allowed variation in the location of the FTT/NAS focus optics must be less than half a micron for a change in ambient temperature of as much as 5 °C.

Our test for this motion utilised a pair of LVDT probes mounted along a diameter of the lens and monitoring the centration of the lens within its aluminium mount while the chamber temperature was changed. The left hand panel of Figure 20 shows this test geometry, together with the locations of the two polymer pins whose expansion/contraction is designed to compensate for the different CTEs of the lens glass and the Aluminium mount (see Sec. 6.2.4 for a discussion of this strategy).

Figure 21 shows the results for a lens shear test where the lens support pins were deliberately fabricated with an incorrect length. Similar tests using other pairs of incorrectly fabricated pins allowed us to determine the correct length needed to give no lens shear as  $16.1 \pm 0.8$  mm. Quite separately we measured the CTE of the pins in a laboratory test set-up. Data from such an experiment, in which length of a pin was measured directly with a precision micrometer as a function of temperature, is presented in Figure 20. These, and other repeat data, were then used to independently compute the pin length needed to keep the lens centred. This gave a value of

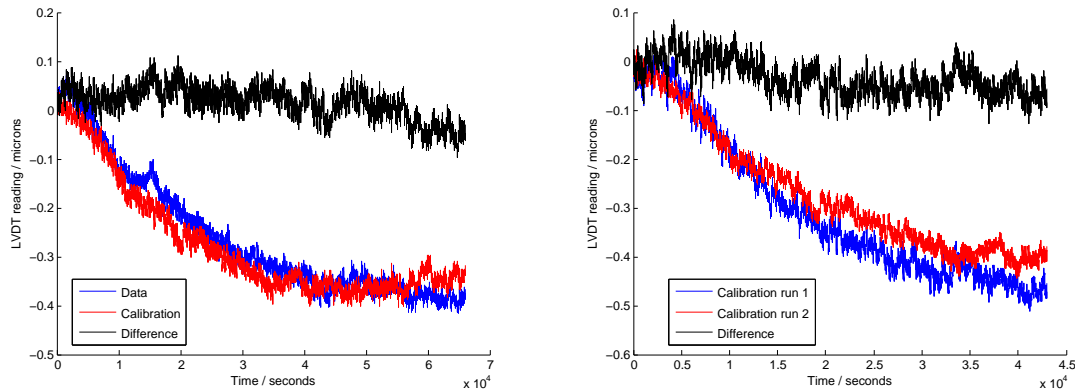


Figure 19: Left: measured (blue and red curves) and calibrated (black curve) LVDT tilt data expressed in microns for a dichroic/fold-mirror mount test. The allowed tilt variation expressed in these units for the temperature change here is 45 nm. Right: equivalent data for two calibration runs. In this case the recovered signal is expected to be zero. The level of residual fluctuations in the black trace is indicative of the level below which calibration errors cannot be eliminated. Overall, these data suggest that the prototype mount may be compliant with its tilt stability requirement, but if it is not, it is unlikely to have exceeded it by more than a factor of two.

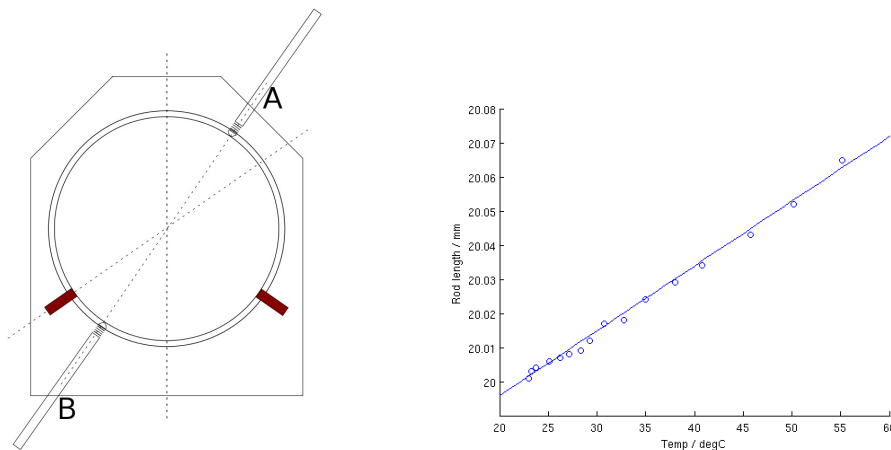


Figure 20: Left: A face-on view of the triplet lens mount showing the LVDT measurement probes in place and the polymer pins that support the lens in the radial direction in red. Right: Measurements of the CTE of one of the polymer rods used for material compensation of the lens centration. The CTE derived for this run was 95  $\mu\text{m}/\text{m}/\text{K}$ . Averaging all runs, the CTE obtained was  $94 \pm 6 \mu\text{m}/\text{m}/\text{K}$ .

16.5  $\pm$  0.9 mm, consistent with the LVDT predictions, and confirming that our material compensation strategy can meet the FTT/NAS requirements. Interestingly, these data suggest that errors in the fabricated lengths of the pins by as much as 1 mm can be tolerated, i.e. the lens motion remain within specification, as long as the CTE of the pin material is known to better than roughly five percent.

A summary of the results of our component mount tests and the desired performance for each mount is presented in Table 6.

<sup>6</sup>In the case of lens shear, the value listed is the movement predicted assuming a 1 mm error in the compensating pin length based on the movements seen with pins of other lengths.

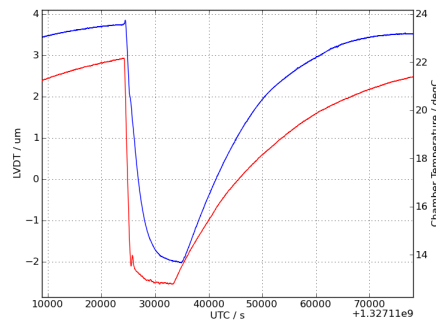


Figure 21: FTT/NAS Lens shear (blue) and chamber temperature (red) as a function of time during a thermal cycle test. In this example, the polymer pins supporting the lens were deliberately fabricated with the incorrect length and so the lens does not remain centred in its mount but moves by roughly one micron per degree Celsius.

Element	Degree of freedom	Measured motion	Required stability	Comments
Dichroic/mirror mount	Piston stability	100 nm	< 500 nm	Compliant
Dichroic/mirror mount	Tilt stability	≤ 100 nm	45 nm	Possibly compliant
Lens mount	Shear stability	≤ 250 nm <sup>6</sup>	~ 350 nm	Compliant

Table 6: Comparison of the FTT/NAS component stability test results and the performance needed to meet the top-level requirements. The dichroic/fold mirror mount tilt stability requirement has been converted into a linear measure associated with the geometry of the experimental set-up.

### 10.2.2 Integrated testing

The focus of our most recent opto-mechanical testing has been to attempt to validate the full optical train of the FTT/NAS. To this end a much larger thermal chamber has been constructed which allows for the full optics baseplate, with optics, to be mounted on an optical table in our laboratory and then be temperature cycled. The walls and base of the chamber are made of 2–2.5 cm thick insulating board and so to first order changes in the internal temperature of the chamber are not transmitted to the external environment<sup>7</sup>. The interfaces between the baseplate and the optical table are identical in concept to those designed for the FTT/NAS but have been fabricated to a slightly lower level of precision.

The design of the chamber, depicted in schematic form in the left hand panel of Figure 22, and shown part assembled in the photograph in the right hand panel, allows for a 9 mm diameter collimated beam from a HeNe laser to be injected along the optical train and be measured on exit from the optical system via a small open port (identified by the number “3” in the figure). This measurement is performed by a CCD camera mounted to the optical table externally and close to its boundary. Similarly, the input beam can also be measured after (i) passing through the dichroic at location “R”; (ii) passing through a semi-silvered fold mirror 1; or (iii) passing through a semi-silvered fold-mirror 2. The rationale for this approach is that, by simultaneously measuring the output beam and, for example, the beam exiting at port R, one can in principle remove the effects of any instabilities in the laser beam injection direction from motions seen in the output beam. Simultaneous measurement of the beams exiting at the other calibration ports are able to assess other types of systematic errors and can help identify which of the components on the base-plate, if any, might be most unstable.

<sup>7</sup>Typically changes in the chamber temperature of 5–10 °C lead to changes in the external temperatures measured in the lab of less than 0.1 °C

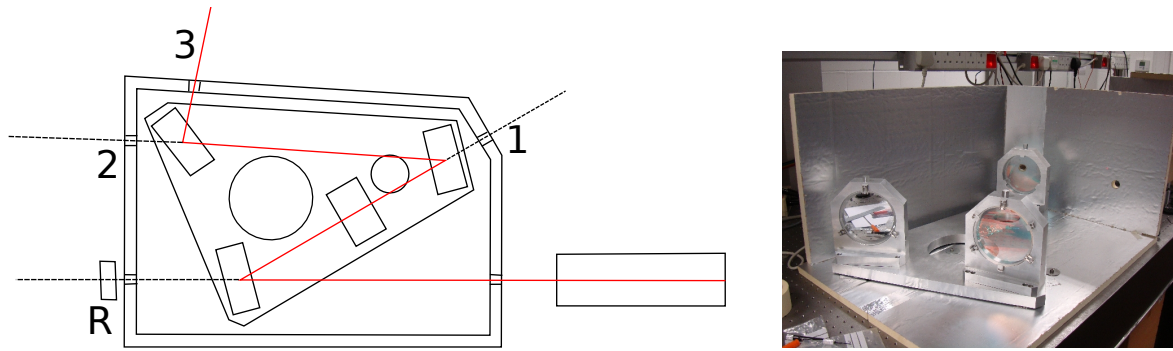


Figure 22: Left: The optical arrangement used for the FTT/NAS integrated test. A collimated laser beam enters from the right, part reflects off the dichroic (at bottom left), passes through the lens and then off the two semi-silvered fold mirrors before exiting at port 3. Ports R, 1 and 2 allow parts of the input beam to be interrogated outside the thermal enclosure after travelling successively longer portions of the optical train. Right: A view of the FTT/NAS optics mounted on their base-plate and enclosed by a partially assembled thermal chamber. The small entrance hole for the input beam can be seen towards the right.

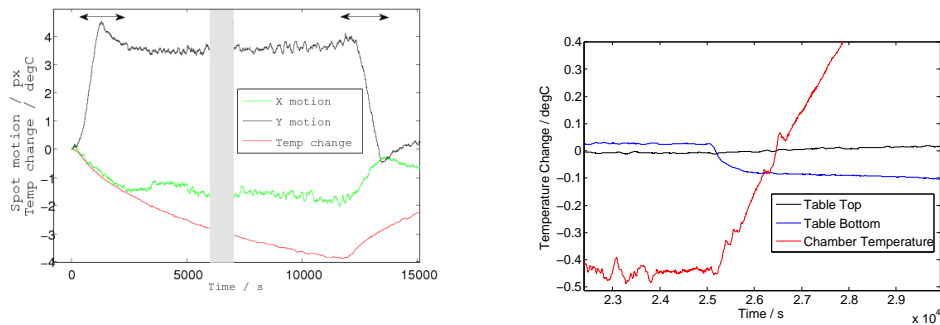


Figure 23: Left: Typical results from an FTT/NAS integrated test showing the “calibrated” motion in x- and y- for a laser beam that has propagated the full optical train. The grey band indicates times at which the data-logger failed. In this experiment the chamber temperature has been dropped by 4 °C and the corresponding allowed image motion is 0.3 pixels. The horizontal arrows show the times at which the largest excursions are seen, and during which the temperature difference between the top and bottom skins of the optical table jumps rapidly. Outside these periods the observed beam motion is approximately at the level of twice the FTT/NAS requirement. Right: The measured temperature of the top and bottom skins of the optical table during a “warm-up”. In these data the water chiller for the thermal chamber was adjusted (at  $T \sim 25,000$  seconds) so as to allow the chamber to slowly rise to ambient conditions. Note the abrupt change in the lower skin temperature which is matched by a much more gradual increase in the upper skin temperature.

The typical sequence for a test was that the chamber was held at room temperature for several hours, and then chilled to roughly 10 °C below ambient over three hours, during which time the output beam as well as one of the “calibration” output beams were monitored. Thereafter, the chamber temperature was allowed to return to the ambient level over a longer period. Tests were usually undertaken overnight so that the laboratory temperature was relatively stable and the conditions otherwise undisturbed.

A typical integrated test result is shown in Figure 23. This shows the “calibrated” exit beam motion — measured in camera pixels, where motions of up to 0.3 pixels are allowed — plotted as a function of time. The chamber temperature is shown by the red trace, and fell by roughly 4 °C over the course of the first three hours of the run. In these data the spot position variations have been corrected for both the observed motions of a calibration

beam exiting at port 1, and the shear in the vertical direction associated with the material compensation of the lens mount. This is because the camera and lens system being used to monitor the exit beam motion is not subject to the temperature changes experienced by the lens mount itself.

The most noticeable features of Figure 23 are the extreme motions of the exit beam direction — the motion in the vertical y-direction is  $15\times$  larger than the allowed budget — at certain times during the experiment. Exhaustive tests have very recently confirmed that these large amplitude motions are exclusively associated with abrupt changes in the temperature difference between the top and bottom skins of the optical table on which the tests are being undertaken. It appears that at key times during the experiments, notably (a) when the cooling cycle is initiated and (b) when active cooling of the chamber is stopped and the temperature of the thermal enclosure is allowed to increase slowly back to ambient, the optical table undergoes a thermal shock and the calibration measurements are compromised. These times are identified by the horizontal arrows in Figure 23 and last no more than an hour. The amplitude of these changes in differential temperature are small, typically no greater than  $0.1\text{ }^{\circ}\text{C}$ , but they appear large enough to compromise our calibration strategy.

We believe that what our data have identified is a warping of the top and bottom optical table surfaces, and resulting changes in the positional and angular orientation of the laser beam and the FTT/NAS baseplate (since the locations of its kinematic seats are altered). The gross effects of the laser beam “wobble” are removed by our calibration strategy, but the apparently much larger effects of any tilting of the FTT/NAS baseplate are not being adequately compensated for.

At other times in the course of the tests, when the differential skin temperature of the optical table is stable, *but importantly while the chamber temperature is changing by several degrees Celsius*, the calibrated spot motion is very stable. During these periods the observed motion is approximately at the level of only twice the FTT/NAS requirement. This is consistent with the results of our individual component mount tests, and indicative that we are very close to meeting the overall FTT/NAS zero-point stability requirement.

In the coming weeks we are intending to continue our integrated tests, with the goals of monitoring any table surface motions directly, and in reducing any cooling-induced temperature shocking of the optical table. We hope to be able to present an update on this aspect of the testing at the time of the PDR.

### **10.3 Thermal testing**

At the time of writing (30th April 2012) we have yet to undertake any thermal testing of the FTT/NAS. In particular we wish to establish how the thermal enclosure for the camera performs in terms of keeping the camera warm (in a cold environment) and also, whether the outer skin of the enclosure will remain within  $2\text{ }^{\circ}\text{C}$  of ambient.

We expect to undertake these measurements once we have completed the integrated opto-mechanical testing of the prototype FTT/NAS.

## **11 Lifetime and Maintenance**

### **11.1 Mechanical components**

Since there are no moving parts or actuators in our preferred preliminary design, there are no life-time issues for components on the optical table. For parts off the optical table, we expect the flow control valve which controls the flow rate of cooling fluid to the camera and camera enclosure to be a manual set valve, and so have few lifetime issues. The air dryer is expected to be a membrane-based unit, which has very low maintenance requirements.

## 11.2 Optical components

The FTT/NAS optical components will be coated as appropriate but these coatings may need cleaning or replacement after several years given their exposed environment in the UT dome.

## 11.3 Electronics components

All electronics components, such as PCs and interfaces, will be sourced with lifetime in mind but the availability of replacement parts cannot be guaranteed. The design has been modularised so that replacement of any one component is made easier by not attempting to combine all interface functions on one multi-purpose board.

## 11.4 Camera

The Andor iXon X3 897 is supplied with a 1 year warranty for most of its hardware, but a longer warranty on the vacuum seal for the detector chamber. We expect there to be no maintenance issues except in keeping the camera window clean and ensuring that there is no corrosion or particulates in the cooling tubes. Faults with the camera or with the vacuum chamber will require the camera to be returned to the manufacturer. Some lifetime issues with e2v EMCCDs exposed to light at high gain have been reported, and we have assessed the test results published by Andor ([http://www.andor.com/pdfs/Longevity\\_in\\_EMCCDs.pdf](http://www.andor.com/pdfs/Longevity_in_EMCCDs.pdf)). In the worst case we are using the gain register a factor 40 times less intensively than in the Andor test and using a factor 4 less gain. Andor measured a lifetime of 7 years for their very aggressive test and we conclude therefore that there are likely to be no such lifetime issues for our application.

## 12 Interfaces

The FTT/NAS interfaces to five major sub-systems, and the FLC to four of these (there is no interface from the FLC to the FTTA). These interfaces are controlled using Interface Control Documents developed by the Cambridge team. Two provisional ICDs existed previously as parts of documentation supplied by other vendors and we have generated an ICD to partner each of these (see Table 7).

We have separated and detailed these interfaces in the set of ICDs developed for the FTT/NA and FLC systems and where the content of an ICD is identical or overlaps for the FTT/NAS and FLC, a single ICD covers both systems. We have developed separate FTT/NAS and FLC ICDs to the ISS since the FLC is expected to implement only a subset of the FTT/NAS commands and data streams. The set of Cambridge-generated interface documents supplied for the PDR are listed in Table 7.

MRO-ICD-CAM-1100-0108 FTT/NAS-FTTA	CAM	Specific FTTA-FTT interface
MRO-ICD-AMO-6000-025 FTTA-FTT	AMOS	General UT electrical ICD
MRO-ICD-CAM-1000-0109 FTT/NAS,FLC-UTE	CAM	FTT/NAS & FLC to Enclosure ICD
MRO-ICD-EIE-0032 UTE-FTT	EIE	Enclosure to FTT system ICD
MRO-ICD-CAM-1000-0110 FTT/NAS,FLC-NOT	CAM	FTT/NAS & FLC to optical table ICD
MRO-ICD-CAM-1000-0111 FTT/NAS,FLC-UT	CAM	FTT/NAS & FLC to UT optical ICD
MRO-ICD-CAM-1100-0112 FTT/NAS-ISS	CAM	FTT/NAS to ISS ICD
MRO-ICD-CAM-1200-0113 FLC-ISS	CAM	FLC to ISS ICD

Table 7: List of FTT/NAS and FLC interface documents.

## 12.1 Specific interface issues

We have resolved the following interface issues since we reported our concerns at the CoDR:

1. Cooling loop 2 (EIE electronics housing) rather than loop 1 has been specified to be routed to a services panel connected to the enclosure wall near the Nasmyth optical table, close to cabinet Q6;
2. Dry air will be routed to the services panel mentioned in (1) where we provide an additional air drying component;
3. The cable route from the FTT/NAS sensor on the optical table to the controller in the electronics housing has been re-calculated from the STP model now that we have established the position of the thermal enclosure on the optical table. The camera cable is 6 m maximum in length and the latest calculation of the route it must take is approximately 5.8 m. This should just leave a sufficient margin for use;
4. The FTT/NAS space envelope issues have been resolved and the applicable drawing modified;
5. The choice of the Andor camera has removed the concern over the power dissipation limitation. However, we request an increase in the allocation from 250 W by 10 W on the rare occasions when the camera enclosure heater needs to be used.

An issue that still remains — and has been verified to some extent by the difficulty we have had in undertaking our integrated system tests in the lab — is the stability of the Nasmyth optical table with changing ambient temperature or thermal loading. This may have an interferometer-wide impact for the FTT/NAS at the MROI and we remind the Project Office that it is likely that the behaviour of the Nasmyth optical table with temperature will limit the extent to which the MROI optical train will remain stable after afternoon/start-of-the-night alignment. A detailed discussion of this topic is beyond the scope of this document, but brief mention of it occurs in Sec. 14.

## 13 Installation Procedure

The optical assembly for the FTT/NAS will be installed from the end of the Nasmyth table close to M4. The camera and service connections will then be installed at the opposite end of the table. The service panel will install underneath the table on the side of the enclosure. All cables will be routed via the ducting directly below the Nasmyth table and travel round to cabinet Q5. The FTT/NAS computer and the 2U electronics rack will be located in the space allocated to them in cabinet Q5.

The outline procedure for the location of the common base-plate of the optical assembly will be as follows:

1. This base-plate will be positioned by direct measurement relative to the axis of the Nasmyth beam (which will have been pre-determined) and the edge of the table closest to the enclosure, taking into account the space envelope defined in the relevant MRO drawing;
2. The defining kinematic seats for the base-plate will then be set in place using measurements of the position of the cone seat and the angle of the parallel bar seat. The flat seat will then be set by relative measurement: its precise location does not have to be accurate;
3. Before fitting, the common base-plate height will be set using its adjustment screws to give a specific height from the Nasmyth table, taking into account the height of the Nasmyth beam axis above the optical table (which will have been pre-determined);
4. The common base-plate will then be fitted onto the kinematic seats. A precision level will be used to check the level of the Nasmyth table and the level of the common base-plate. A straight-edge will be

used to project the surface of the base-plate to the location of the camera mount and the height of this with respect to the Nasmyth table will be checked. Based on these measurements the tilt of the common base-plate will be adjusted if necessary to take account of any non-flatness of the Nasmyth table affecting the locations of the kinematic seats or camera position;

5. The camera position will initially be set by dead reckoning and its steel base-plate (with embedded kinematic seats) will be positioned relative to the common base-plate. Since the camera base-plate clamps to the optical table it will be easy to re-position it. Precision screw blocks that mount to the optical table will be provided for controlled movements, in particular to achieve accurate focus of the camera;
6. As a check on alignment it will be possible to set a laser up on the Nasmyth beam axis using simple targetry before mounting the FTT system. The beam from this can be propagated through to the camera position and its location on the FTT/NAS sensor can be checked by reading out the camera.

## 14 Performance Evaluation

In this section we compare the performance requirements for the FTT/NAS with the performance predicted for the design and determine whether the requirements are likely to be met. In the case where the requirements are not likely to be met, we evaluate the impact of not meeting the requirement on the MROI system performance.

### 14.1 Zero-point stability

Requirement 58 in RD1 states that:

*Any changes in the beam direction in the BCA that corresponds to the tip-tilt zero-point (e.g. due to tilt or position drifts of optical components on the UT Nasymth table) since start-of-night calibration shall not exceed 0.015 arcsec on the sky, for changes in ambient temperature up to 5 °C. In assessing compliance with this requirement, the FTT/NAS supplier should assume that the UT Nasmyth table is perfectly stable.*

The opto-mechanical component stability tests presented in Sec. 10 show that all components meet their allocated error budgets, except for the tilt stability of the dichroic/fold-mirror mounts, which *in the worst case* may exceed the tilt error specification by a factor of two<sup>8</sup>. If we assume that fold mirror mounts have the same stability as the dichroic mount and all the other degrees of freedom meet their error budget targets, then the total error budget for the stability of the tip/tilt zero point is exceeded by a factor of approximately 1.7 in this worst case.

The effect of exceeding the allowed stability margin will be to reduce the interferometric fringe visibility due to relative tilts of the interfering beams. For a relative tilt offset of two beams by an amount  $\theta$  then the visibility of the fringes will be decreased by a factor

$$\gamma = 1 - (\pi\theta D/\lambda)^2/8, \quad (1)$$

where  $D$  is the beam diameter and  $\lambda$  is the wavelength of the interfering beams. For  $\lambda = 1.6 \mu\text{m}$  and  $D = 1.4 \text{ m}$ , then, assuming that the typical relative tilt of two beams is  $\sqrt{2}$  times the drift of the individual beams, then a single-beam drift of 0.015 arcsec will lead to a visibility loss of 1%, whereas exceeding this value by a factor of 1.7 will cause a visibility loss of roughly 3%.

---

<sup>8</sup>These mounts may perform better than this, but, as reported, our current component mount tests are unable to measure tilt motions any smaller than approximately two times the stability requirement.

This potentially changing visibility loss will cause both calibration errors and also a signal-to-noise loss equivalent to a throughput loss of approximately 6%.

These effects, coupled with the fact that the tilt of the Nasmyth table is likely to be unstable at a much greater level than this, argues very strongly for the use of some form of mechanism that can compensate in real time for drifts such as these, caused by slowly creeping optical components. The BEASST system at MROI is designed for just this purpose, and is aimed at monitoring and correct any tilt and shear errors in the beams arriving in the inner BCA due to, e.g. optics whose mounts are creeping as the ambient conditions change.

An estimate of how fast BEASST would need to operate in order to keep the effect of the drifts in the FTT/NAS components within tolerance can be obtained by assuming that the drifts are linear with temperature. In this case the FTT components would cause a drift out of tolerance for a temperature change of approximately  $5\text{ }^{\circ}\text{C}/1.7 = 3\text{ }^{\circ}\text{C}$ .

At a typical rate of change of ambient temperature of  $1.5\text{ }^{\circ}\text{C}/\text{h}$  then a drift compensation system would need to operate at least every 90–120 minutes in order to keep the tilt drift within tolerance. This assumes that the FTT/NAS optics were the only source of tilt drift, which is rather unlikely. Fortunately, the BEASST system is specified to update at rates of many times per hour and so should easily be able to cope with this.

Our experience with our lab optical table “warping” with changes in differential skin temperature confirms that much larger drifts in the zero-point position are possible — many tens of times the requirement over timescales of an hour. However, while it is likely that such large amplitude table deformations will occur at the MROI site, they will likely take place more slowly since in our experiments it appears that it is our test apparatus itself that is driving the perturbations.

## 14.2 Closed-loop bandwidth

Sec. 10.1 notes that the latency of the camera and computing system is likely to be sufficient to implement robust closed-loop operation with a bandwidth of 43 Hz. This exceeds the requirement for a bandwidth of 40 Hz, but does not meet the goal of 50 Hz. Not meeting the goal could lead to a loss of fringe contrast and hence interferometric sensitivity on nights of poor seeing, but the sensitivity will be low on such nights anyway. Thus not meeting the goal has a minimal impact on the science capabilities of the array.

## 14.3 Limiting sensitivity

Sec. 2 shows that the required throughput for meeting the allowed residual jitter on a 16th magnitude AGN is greater than 100%, given certain assumptions about the implementation. Sec. 4.3 shows that the estimated throughput of the designed system is predicted to be 86% and Sec. 10.1 reports that it is likely that the Andor EMCCD camera can be operated satisfactorily in a fast-frame-rate mode with a gain of 250, thus minimising the effects of read noise. As a result, the system will not meet the limiting magnitude requirement but will not be far off: instead of meeting the residual jitter requirement at a magnitude of 16.0 it will meet it for a source of magnitude 15.8.

The requirement might still be met by using different centroiding algorithms, for example correlation algorithms, which give lower centroiding errors at 16th magnitude, but this needs to be investigated further. Also, the residual jitter from the telescope used in the calculation is an upper limit, so the actual jitter observed may be less than predicted.

At a magnitude of 16.0, the calculated residual tilt jitter will be some 2% over budget, resulting in a 0.5% visibility loss in the fringe tracker at H-band. This loss in visibility should only result in a small fraction of candidate targets being unobservable in the reference seeing conditions due to the fringe-tracking SNR being

too low. An equivalent way of saying this is that for only a 0.25% improvement in seeing conditions, all the candidate targets should be observable.

## 14.4 Mass budget

We exceed our mass budget by approximately 27 kg. The implication of this is that the Nasmyth optical table will have a slightly lower resonant frequency. An estimate of the reduction in frequency can be made by comparing the total mass of the table and assemblies on it, with the additional mass: these figures are 345 kg and 27 kg respectively. The mass increase is 7.8% and so the natural frequency will be lowered by 2.8% or approximately 2 Hz for a 70 Hz natural frequency. The impact of this reduction in eigenfrequency is thus likely to be negligible and in any case would not be realised until the table were populated with an AO system.

## 15 Conclusions

We have presented a comprehensive design for the FTT/NA system together with test results which allow us to predict the expected system performance. We expect to be compliant with the performance requirements (marginally compliant in the case of limiting sensitivity), with the exception of opto-mechanical stability. There are ambiguities in interpreting the integrated test results we have obtained thus far, but we believe the results are consistent with the component test results which indicate that we will exceed the zero-point stability requirement by a factor of roughly 2. If left uncorrected, such zero-point drifts would have a moderate impact on the limiting sensitivity (equivalent to 6% throughput loss) and calibration accuracy of MROI. We hope to present improved integrated test results on the day of the PDR.

The experimental difficulties we encountered with the integrated test have highlighted the fact that the Nasmyth table will most likely be unstable at many times the level of the FTT/NAS requirement, and so the BEASST system will be needed to sense and compensate for these drifts if realignment during the night is to be avoided. BEASST will take out both the Nasmyth table effects and the drifts of the FTT/NAS opto-mechanics, and we have established that the latter drifts are slow enough that they can be fully corrected using BEASST.

We are not proposing any adjustments to our designs in an attempt to improve the opto-mechanical stability. We believe that any such improvements would be costly, both in terms of design cost and manufacturing cost if e.g. invar were used, and that any improvements made would be extremely difficult to measure in a conventional laboratory environment. Furthermore, such efforts would be negated by the impact of the Nasmyth table instabilities.

Therefore we propose to proceed with refinement and manufacture of our current design according to the schedule set out in our change order request of 15 February 2012. Procurement and manufacture of the opto-mechanical components and camera thermal enclosure would be done in parallel with continued software development. These activities would come together in the setting up of a closed-loop laboratory demonstration that will correct artificially-generated fast tip-tilt perturbations.

The remaining FLC components will also be manufactured in parallel with the above activities, to be completed by August 2012. The majority of the FLC software functionality has already been realised, and we anticipate that a first release of the FLC software could be made in a few months from now.

### 15.1 Software

The design of all components of the FTT/NAS software is essentially complete, including definition of the system properties, commands, and monitor points that comprise the interface to the ISS. Coding of the system controller and control/display GUI is well advanced, and a precursor to the environment controller is complete

and has been used extensively for our opto-mechanical stability tests. Aspects of the analysis GUI have been successfully prototyped.

We believe we have already mitigated the major technical risks associated with the software. The real-time performance of the code has been demonstrated, and we have shown by simulation that a candidate fast tip-tilt correction algorithm can meet the limiting sensitivity requirement (with potential improvements to the algorithm yet to be tried).

The current version of our software is based on a preliminary standalone version of the MROI Generic System Interface framework. We are expecting a number of changes to the GSI over the coming weeks and months. The uncertainties in the timescale and content of these changes may lead to an impact on the schedules for delivering the FLC and FTT releases of the software. However, the availability of the alternative dlmsg interface for controlling the system and capturing test data will allow many tasks to proceed (in particular the closed-loop laboratory demonstration) while the GSI framework is in flux.

## 15.2 Schedule and prospects

The deliverables and expected completion dates for the current contract are as follows (these are unchanged from the February 15th 2012 change order):

- WBS-04-001** Optical component mount rework & test – 15 Sep 2012
- WBS-04-002** Camera enclosure manufacture – 1 Aug 2012
- WBS-04-003** Optics procurement – Orders to be placed by 1 Jun 2012
- WBS-04-004** Fast tip-tilt mode software – 15 Sep 2012
- WBS-04-005** Integrated stability testing – 1 Nov 2012
- WBS-04-006** Closed-loop system testing (to verify functionality) – 1 Nov 2012
- WBS-4-007** Test Report – 15 Nov 2012

As a near-term task, we need to agree specifications for the preliminary dichroic coating and for the corner cube optic with the MROI Project Office. We can then proceed with these procurements.

The subsequent tasks that would lead to delivery and acceptance of a fully-functional FTT/NA system are principally:

- Further closed-loop system testing to verify performance;
- Completion of FTT/NAS software (ISS interface to fast tip-tilt mode and optimization of algorithms);
- Execution of factory and site acceptance tests.

As we are not proposing significant revisions to our current designs, the most recent estimates we provided for the cost and schedule to deliver the first FTT/NA system are still valid (subject to small adjustments depending on the rate at which funding can be provided by MRO).

We believe there to be a very low level of technical risk going forwards. We have already demonstrated an acceptable level of performance by means of our preliminary design phase testing efforts. The remaining uncertainties concern the availability of revised versions of the Generic System Interface software framework and the risk of consequent delays in integrating the FTT/NAS software with the ISS, and some details of the software algorithms which have yet to be investigated.

In conclusion, we request that the MRO Project Office allow us to proceed with the current designs according to the previously-agreed schedule. We look forward to the eventual delivery of the system to the Magdalena Ridge and its successful integration into the interferometer.